ARMY RESEARCH LABORATORY

Modeling Dislocations and Disclinations With Finite Micropolar Elastoplasticity

by John D. Clayton, David L. McDowell, and Douglas J. Bammann

ARL-RP-120 **February 2006**

A reprint from the *International Journal of Plasticity*, vol. 22, pp. 210–256, 2006.

NOTICES

Disclaimers

The findings in this report are not to be construed as an official Department of the Army position unless so designated by other authorized documents.

Citation of manufacturer's or trade names does not constitute an official endorsement or approval of the use thereof.

Destroy this report when it is no longer needed. Do not return it to the originator.

Army Research Laboratory
Aberdeen Proving Ground, MD 21005-5066

ARL-RP-120 **February 2006**

Modeling Dislocations and Disclinations With Finite Micropolar Elastoplasticity

John D. Clayton
Weapons and Materials Research Directorate, ARL

David L. McDowell
Georgia Institute of Technology

Douglas J. Bammann
Sandia National Laboratories

A reprint from the *International Journal of Plasticity*,
vol. 22, pp. 210–256, 2006.

REPORT DOCUMENTATION PAGE

Form Approved
OMB No. 0704-0188

1. REPORT DATE *(DD-MM-YYYY)*	2. REPORT TYPE	3. DATES COVERED (From - To)
February 2005	Reprint	1 January 2003–1 January 2006

4. TITLE AND SUBTITLE
Modeling Dislocations and Disclinations With Finite Micropolar Elastoplasticity

5a. CONTRACT NUMBER

5b. GRANT NUMBER

5c. PROGRAM ELEMENT NUMBER

6. AUTHOR(S)
John D. Clayton, David L. McDowell,[*] and Douglas J. Bammann[†]

5d. PROJECT NUMBER
1L1622618AH80

5e. TASK NUMBER

5f. WORK UNIT NUMBER

7. PERFORMING ORGANIZATION NAME(S) AND ADDRESS(ES)
U.S. Army Research Laboratory
ATTN: AMSRD-ARL-WM-TD
Aberdeen Proving Ground, MD 21005-5066

8. PERFORMING ORGANIZATION REPORT NUMBER
ARL-RP-120

9. SPONSORING/MONITORING AGENCY NAME(S) AND ADDRESS(ES)

10. SPONSOR/MONITOR'S ACRONYM(S)

11. SPONSOR/MONITOR'S REPORT NUMBER(S)

12. DISTRIBUTION/AVAILABILITY STATEMENT
Approved for public release; distribution is unlimited.

13. SUPPLEMENTARY NOTES
A reprint from the *International Journal of Plasticity*, vol. 22, pp. 210–256, 2006.
[*]George W. Woodruff School of Mechanical Engineering, Georgia Institute of Technology, Atlanta, GA 30332-0405.
[†]Department of Science-based Materials Modeling, Sandia National Laboratories, Livermore, CA 94550.

14. ABSTRACT
Aspects of a constitutive model for characterizing crystalline metals containing a distribution of dislocation and disclination defects are presented. Kinematics, balance laws, and general kinetic relations are developed – from the perspective of multiscale volume averaging – upon examination of a deforming crystalline element containing a distribution of displacement discontinuities in the form of translational and rotational lattice defects, i.e., dislocations and disclinations. The macroscopic kinematic description is characterized by a three-term multiplicative decomposition of the deformation gradient. The micro-level description follows from an additive decomposition of an affine connection into contributions from populations of dislocations and disclinations to the distortion of the lattice directors. Standard balance equations apply at the macroscopic scale, while momentum balances reminiscent of those encountered in micropolar elasticity (i.e., couple stress theory) are imposed at the micro-level on first- and second-order moment stresses associated with geometrically necessary defects. Thermodynamic restrictions are presented, and general features of kinetic relations are postulated for time rates of inelastic deformations and internal variables. Micropolar rotations are incorporated to capture physics that geometrically necessary dislocations stemming from first-order gradients of elastic or plastic parts of the total deformation gradient may alone be unable to reflect, including evolution of defect substructure at multiple length scales and incompatible lattice-misorientation gradients arising in ductile single crystals subjected to nominally homogeneous deformation.

15. SUBJECT TERMS
constitutive behavior, crystal plasticity, disclinations, dislocations, microstructures

16. SECURITY CLASSIFICATION OF:			17. LIMITATION OF ABSTRACT	18. NUMBER OF PAGES	19a. NAME OF RESPONSIBLE PERSON
a. REPORT	b. ABSTRACT	c. THIS PAGE			John D. Clayton
UNCLASSIFIED	UNCLASSIFIED	UNCLASSIFIED	UL	54	19b. TELEPHONE NUMBER (*Include area code*) (410) 306-0975

Available online at www.sciencedirect.com
SCIENCE DIRECT®
International Journal of Plasticity 22 (2006) 210–256
INTERNATIONAL JOURNAL OF Plasticity
www.elsevier.com/locate/ijplas

Modeling dislocations and disclinations with finite micropolar elastoplasticity

J.D. Clayton [a,*], D.L. McDowell [b], D.J. Bammann [c]

[a] *Impact Physics Branch, U.S. Army Research Laboratory, Aberdeen Proving Ground, MD 21005-5069, USA*
[b] *George W. Woodruff School of Mechanical Engineering, Georgia Institute of Technology, Atlanta, GA 30332-0405, USA*
[c] *Department of Science-based Materials Modeling, Sandia National Laboratories, Livermore, CA 94550, USA*

Received 1 July 2004
Available online 11 April 2005

Abstract

Aspects of a constitutive model for characterizing crystalline metals containing a distribution of dislocation and disclination defects are presented. Kinematics, balance laws, and general kinetic relations are developed – from the perspective of multiscale volume averaging – upon examination of a deforming crystalline element containing a distribution of displacement discontinuities in the form of translational and rotational lattice defects, i.e., dislocations and disclinations. The macroscopic kinematic description is characterized by a three-term multiplicative decomposition of the deformation gradient. The micro-level description follows from an additive decomposition of an affine connection into contributions from populations of dislocations and disclinations to the distortion of the lattice directors. Standard balance equations apply at the macroscopic scale, while momentum balances reminiscent of those encountered in micropolar elasticity (i.e., couple stress theory) are imposed at the micro-level on first and second order moment stresses associated with geometrically necessary defects. Thermodynamic restrictions are presented, and general features of kinetic relations are postulated for time rates of inelastic deformations and internal variables. Micropolar rotations are incorporated to capture physics that geometrically necessary dislocations stemming from first

* Corresponding author. Fax: +1 410 306 0783.
E-mail address: jclayton@arl.army.mil (J.D. Clayton).

0749-6419/$ - see front matter
doi:10.1016/j.ijplas.2004.12.001

order gradients of elastic or plastic parts of the total deformation gradient may alone be unable to reflect, including evolution of defect substructure at multiple length scales and incompatible lattice misorientation gradients arising in ductile single crystals subjected to nominally homogeneous deformation.

Keywords: Constitutive behavior; Crystal plasticity; Disclinations; Dislocations; Microstructures

1. Introduction

Processes of grain subdivision and dislocation substructure formation are known to substantially affect slip system activity, strain hardening, stored lattice energy, and texture evolution in single crystals and polycrystals (Hughes et al., 1997, 2003; Kuhlmann-Wilsdorf, 1999; Butler et al., 2000; Barton and Dawson, 2001; Hughes, 2001; Leffers, 2001). Also measured within pure ductile metals and certain alloys at large deformations and/or high temperatures are long range internal stress fields associated with misoriented subgrain boundaries (Gibeling and Nix, 1980; Argon and Takeuchi, 1981); moreover, recent experiments on cyclic dislocation cell structures (Kassner et al., 2002) suggest such internal stress fields may be of negligible magnitude in the macroscopically unloaded configuration in FCC crystals. The trend in many metallic systems of increasing strength with decreasing size of considered volume or microstructural features is also well known. Perhaps most often cited in this context is the Hall–Petch relation, in which yield stress and cleavage strength increase with decreasing grain size in polycrystals (Hall, 1951; Petch, 1953). Since polycrystalline grain boundaries and deformation-induced internal boundaries share certain fundamental characteristics such as lattice incompatibility (i.e., misorientation across interfaces) and nominally large defect densities relative to the bulk material, one would expect some degree of similarity in the effects engendered by these boundaries upon homogenized mechanical properties of the material such as macroscopic strength and hardness.

Composite models wherein walled cellular dislocation structures, represented by hard and soft regions of relatively high and low defect densities, respectively, have been suggested to explain the effects of evolving populations of these substructures on flow stress (Mughrabi, 1983, 1988, 2001; Berveiller et al., 1993; Zaiser, 1998). Meyers and co-workers (Meyers and Ashworth, 1982; Benson et al., 2001; Fu et al., 2001) invoked composite models featuring grain boundary layers of relatively high dislocation density to explain grain size influences on yielding. Formulations have also been proposed that explicitly embed subdivision and related dislocation substructure effects into the kinematics of crystal plasticity theory (Leffers, 1994; Butler and McDowell, 1998) and the hardening and intergranular interaction laws of polycrystalline models (Horstemeyer and McDowell, 1998; Horstemeyer et al., 1999). Composite micromechanics models have also been applied to describe the breakdown of the Hall–Petch effect in nanocrystalline solids (Capolungo et al., 2005).

A great many continuum treatments of elasticity or elastoplasticity include enhancements intended to describe influences of microstructure on the mechanical response of the material, perhaps beginning with the pioneering director theory of Cosserat and Cosserat (1909). Multi-polar and higher gradient elasticity theories featuring higher order stresses (e.g., couple stresses) were developed by Truesdell and Toupin (1960), Toupin (1962, 1964), Green and Rivlin (1964), Teodosiu (1967), and Eringen (1972), among others. Kröner (1963) explained the origin of couple stresses from a volume averaging perspective, with the Cauchy stress for a representative volume containing uniformly distributed lattice defects defined as the average of the microscopic stress, and the couple stresses produced by fluctuations in the microscopic stress fields induced by the defects. Early strain gradient plasticity theories were postulated by Fox (1968), Teodosiu (1969), Lardner (1969), Dillon and Kratochvíl (1970), and Dillon and Perzyna (1972). Holt (1970) and Bammann and Aifantis (1982) developed gradient-based models of dislocation kinetics. Kröner (1973) and Hartley (1975) considered the effects of higher order moments of dislocation distributions. By statistical averaging of elastic stress fields imparted by distributions of discrete dislocation dipoles, Groma et al. (2003) derived continuum expressions for resistance to plastic deformation, with flow stresses (due to shorter-range dislocation force interactions) depending upon the average dislocation density and back stresses (due to longer-range interactions) depending upon the first spatial gradient of the dislocation density. In recent years, higher order plasticity theories have exhibited a resurgence in popularity, as evidenced by an abundance of models featured in the literature (cf. Aifantis, 1987; Fleck and Hutchinson, 1993; Nagdhi and Srinivasa, 1993; Fleck et al., 1994; Le and Stumpf, 1996a; Shizawa and Zbib, 1999; Acharya and Bassani, 2000; Acharya, 2003; Bammann, 2001; Regueiro et al., 2002; Gurtin, 2002; Svendsen, 2002; Garikipati, 2003; Clayton et al., 2004a). The fundamental kinematic descriptions invoked by many of these theories are based upon differential-geometric foundations often credited to Bilby et al. (1955), Günther (1958), Kröner (1960), Kondo (1964), Truesdell and Noll (1965), and Noll (1967), while the concept of compatibility-maintaining geometrically necessary dislocations was established by Nye's tensorial description (1953) and then popularized by Ashby's (1970) seminal paper. Higher order plasticity theories have been used to explain grain size effects upon hardness or flow stress (Shu and Fleck, 1999; Evers et al., 2002), to predict geometrical characteristics of deformation bands (Aifantis, 1987; Gurtin, 2000), to provide insight into dislocation nucleation criteria (Acharya, 2003), and to alleviate mesh dependency issues in numerical implementations (cf. Menzel and Steinmann, 2000).

It should be noted that in the majority of the above gradient-type theories, geometrically necessary dislocations representing defect substructure will not evolve in single crystals subjected to nominally homogeneous boundary and initial conditions; in these theories, stress and elastic deformation gradient fields will remain spatially constant within regions of a single crystal subjected to such boundary conditions unless the constitutive formulation favors development of deformation heterogeneity, for example from the standpoint of material instability. By homogeneous boundary conditions we mean linear displacement or constant traction applied to the external

surface of the single crystal, along with any higher order boundary conditions – often necessitated by the presence of strain gradients in the formulation, for example – that would result in null lattice curvature on the boundary. Correspondingly, homogeneous initial conditions imply no initial lattice curvature or gradients in initial hardness within the crystal. Kratochvíl and Orlová (1990) and Sedláček et al. (2001) addressed self-organization of dislocation substructure using nonlinear stability analyses. Ortiz and co-workers (Ortiz and Repetto, 1999; Ortiz et al., 2000) constructed a nonlocal lamination theory for modeling additional internal degrees of freedom associated with dislocation substructure, with kinetics dictated by minimization of the incremental work of deformation arising from a non-convex strain energy potential that admits multiple quasi-stable states. Similarly, Carstensen et al. (2002) remarked how heterogeneous plastic flow may result from a lack of convexity of the free energy when evolution of deformation is viewed from the standpoint of a constrained energy minimization problem. Possible sources of instability or non-convexity of the strain energy density of single crystals, from the perspective of continuum plasticity theory, include geometrical softening and strong latent hardening (Ortiz and Repetto, 1999; Sedláček et al., 2001; Carstensen et al., 2002). Such lack of convexity is thought to promote subdivision of crystals into subdomains characterized by single slip and varying gradients of deformation, analogous to the minimum energy configurations postulated for microstructural refinement in the crystallographic theory of martensite (Ball and James, 1987; Bhattacharya, 1991).

In the present work we appeal to the mathematical concept of a *disclination* to describe rotational defects in crystals. In a general sense, such defects may include low angle, high angle, and twin boundaries. In essence, disclinations embody equivalent arrays of dislocations with net Burgers vectors that can also be used to represent these boundaries. Limiting these boundaries to finite strain energy necessitates that they be composed of disclinations of finite size, i.e., partial disclinations bounded by walls of disclination dipoles, termed disclination structural units by Nazarov et al. (2000). The principal reason we seek to extend finite elastoplasticity to incorporate disclinations is that such defects convey important implications with regard to size effects and self-organization of dislocation substructure which are becoming increasingly evident in experimental characterization at finer length scales (Pantleon, 1996; Hughes et al., 1998; Kassner and Pérez-Prado, 2000; Valiev et al., 2002). By including both dislocations and disclinations in our framework, we are able to distinguish between geometrically necessary defect densities reflecting lattice incompatibilities at multiple length scales (i.e., multiple characteristic spacings). For example, Hughes and co-workers (Hughes et al., 1997, 1998; Hughes and Hansen, 2000; Hughes, 2001) have observed within deforming ductile FCC metals the formation of cells of relatively small misorientation organized collectively into larger cell blocks, with average misorientations between blocks usually significantly greater in magnitude than those between cells. Upon increasing applied strain, cell block sizes generally decrease at faster rate than do cell sizes (Hughes et al., 1997). In the context of our theory, the disclination concept can be used to capture the gradients of lattice rotation at the cell block boundaries that arise from the organization and superposition of relatively small misorientations between the cells, reflected here by

geometrically necessary dislocations. Additionally, when the kinetics of evolution of statistically stored defects, geometrically necessary dislocations, and geometrically necessary disclinations are properly coupled, cells and cell blocks will emerge in single crystals upon homogeneous loading, as observed in the aforementioned experiments, and the subdivided crystal will attain an energetically favorable configuration (i.e., a local minimum in free energy over its entire volume). We suggest that a lack of local convexity – or, more precisely, lack of "cross-quasiconvexivity" in the terminology of Carstensen et al. (2002) – stems from the superposition of free energy wells associated with different mechanisms, in our case associated with generation and interaction of defect densities of various origins (e.g., populations of geometrically necessary and statistically stored dislocations and disclinations). This concept is demonstrated explicitly in Appendix A of the present paper.

Some brief descriptive remarks regarding disclination defects are now in order. In the early twentieth century, Volterra (1907) introduced six fundamental types of defects in elastic bodies: three types of translational displacement discontinuities, known as edge and screw dislocations, and three types of rotational incompatibilities, later termed disclinations by Frank (1958) and further classified as either wedge or twist disclinations (see Fig. 1). Disclination theory has been applied to numerous problems of interest. These include descriptions of micropolar rotations in liquid crystals (cf. Frank, 1958; Cermelli and Fried, 2002), rotational defect substructures and commensurate strain hardening in metal forming processes (Romanov, 1993; Seefeldt and Klimanek, 1997, 1998; Valiev et al., 2002), grain boundary structure in Bravais crystals (Li, 1972; Gertsman et al., 1989; Nazarov and Romanov, 1989; Rybin et al., 1993), deformation twins (Müllner and Romanov, 1994), and polycrystalline triple junctions (Bollmann, 1991). Disclinations have also been recognized as characteristic defects in polymers (Li and Gilman, 1970) and nanocrystals (Nazarov

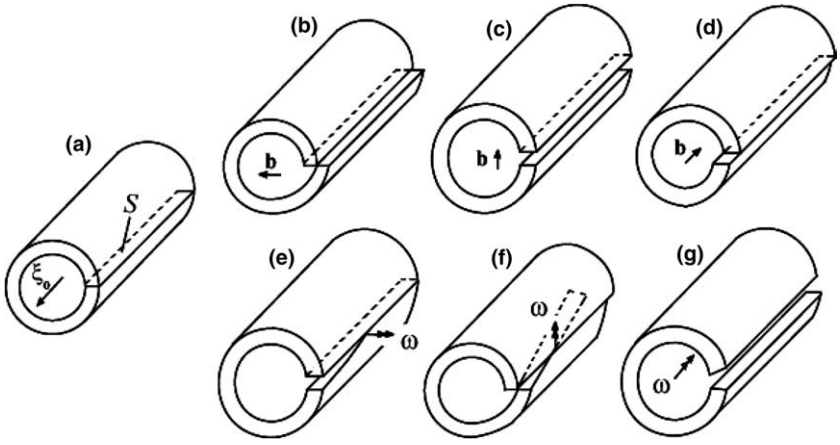

Fig. 1. Volterra's defects: (a) reference cylinder with defect line ξ_0 and cut surface S; (b,c) edge dislocations and (d) screw dislocation with Burgers vector $\mathbf{b}$; (e,f) twist disclinations and (g) wedge disclination with Frank vector $\boldsymbol{\omega}$.

et al., 1993; Konstantinidis and Aifantis, 1998). Molecular dynamics simulations incorporating disclination concepts (Shenderova and Brenner, 1999; Nazarov et al., 2000) have been undertaken to characterize grain boundary energy distributions over a range of intergranular misorientations.

Continuum theories of distributed dislocations and disclinations can be found in the geometrically oriented papers of Anthony (1969), Eringen and Claus (1970), Lardner (1973), Kossecka and de Wit (1977), Minagawa (1977, 1979, 1981), Amari (1981), and De Wit (1981). The texts of Nabarro (1967), Lardner (1974), Mura (1982), Maugin (1993), and Zubov (1997) also include precise mathematical descriptions and/or elastic solutions. De Wit (1973) developed a theory of distributed disclination loops. Pęcherski (1983, 1985) employed disclination concepts in continuum formulations describing finite elastoplastic kinematics, strain hardening, dislocation substructure development, and geometrical softening, the latter resulting from local lattice rotations and acting as a potential precursor to shear localization. An extensive review of disclination theory focusing upon defect kinetics and contributions to plastic strain hardening was provided by Seefeldt (2001), who suggested that partial disclination dipoles be used to describe the collective effects of dislocations comprising misoriented subgranular interfaces (i.e., cell block boundaries), manifesting dislocation substructure refinement in advanced stages of plastic deformation. Seefeldt et al. (2001a,b) used dislocation–disclination models to predict texture diffusion and cellular refinement commensurate with grain subdivision. Panin (1998) and Makarov et al. (1999) emphasized the role of disclination structures accompanying finite inelastic rotations at the mesoscale, often occurring in conjunction with shear localization triggered by microscopic heterogeneity. Lazar and Maugin (2004) recently described the stress field of a wedge disclination via higher gradient elasticity theory.

Classification of disclinations as fundamental defects in Bravais crystals has been an occasional subject of debate in the literature (Kröner, 1983; Marcinkowski, 1990; Kröner and Lagoudas, 1992). This argument arises because one generally must consider a larger length scale of observation (e.g., the vector $\mathbf{r}$ from the axis of rotation to the point of discontinuity) to define the net displacement jump associated with a single disclination in a Bravais crystal (Kondo, 1964; Romanov, 1993) than is required for an isolated dislocation, whose effects manifest at a scale on the order of the lattice parameter. In fact, one may generally construct an equivalent lattice configuration by replacing disclinations with organized arrays of translational dislocations (Li, 1972; De Wit, 1981; Kröner, 1983; Marcinkowski, 1990; Seefeldt, 2001). While such a reconstruction in terms of dislocations may be capable of capturing exactly the stress fields associated with the original distribution of disclinations, the lattice curvature may not always be so well reproduced (De Wit, 1981). It should be noted that partial disclinations are needed to describe lattice misorientations of strength less than 90° in a cubic lattice (60° in a hexagonal lattice), and disclination dipole descriptions are generally required to allow termination of misoriented interfaces over finite distances, providing for bounded elastic energies (De Wit, 1971, 1981; Seefeldt, 2001).

Fig. 2 demonstrates how a simple tilt boundary may be represented either in terms of dislocations or partial disclination dipoles (Li, 1972). In Fig. 2, φ is the angle of

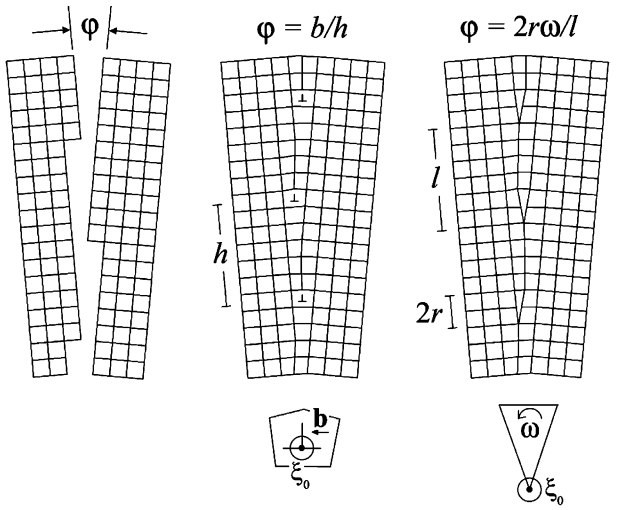

Fig. 2. Tilt boundary (left) comprised of edge dislocations (center) or partial disclination dipoles (right).

misorientation, b is the magnitude of the Burgers vector, ω is the magnitude of the Frank vector (i.e., the strength of the individual disclination), h is the spacing between edge dislocations, l is the spacing between disclination dipoles, and $2r$ is the characteristic spacing between partial wedge disclinations comprising each disclination dipole. Pure twist boundaries may be constructed from either screw dislocations or partial twist disclination dipoles in an analogous fashion (Seefeldt, 2001), and general grain boundaries – including all types of coincident-site interfaces such as deformation twins – can be built up from a mixture of dislocation or disclination types. A certain amount of stored energy is associated with the stacking fault produced by each partial disclination, analogous to the stacking fault energy associated with partial dislocations. Li (1960, 1972) demonstrated for an isotropic linear-elastic solid the equivalence between the strain energy density of a wedge disclination dipole and a finite wall of edge dislocations. We note that for general boundaries, while a suitable representation of the lattice configuration at the microscopic level in terms of discrete dislocations alone is always possible, we find the disclination concept a useful vehicle for engendering additional degrees-of-freedom to our continuum theory to distinguish and isolate the role of long range, cooperative defects in accommodation of lattice strain and curvature.

In the present paper we develop a continuum theory of finite elastoplasticity for crystalline metals containing continuous distributions of dislocation and disclination defects. Our theory distinguishes, in a novel manner, between kinematic and energetic contributions from geometrically necessary dislocations attributed to heterogeneous plastic deformation fields and disclination-type boundary structures associated with initial and evolving subgranular lattice orientation gradients. A three-term multiplicative decomposition of the deformation gradient is suggested in Section 2 following examination of a deforming crystalline volume element

containing ensembles of lattice defects. A linear connection describing spatial variations in the configuration of a triad of lattice director vectors is introduced, consisting of contributions of stretch and rotation from the macroscopic lattice deformation field and micropolar degrees-of-freedom that capture additional lattice rotation due to disclinations. Standard methods of differential geometry are employed to construct the density tensors of geometrically necessary dislocations and disclinations, with the former accommodating incompatible elastic (or plastic) deformation gradients associated with heterogeneity of dislocation glide, and the latter capturing additional misorientations across subgrain boundaries, for example. In Section 3, we outline fundamental balance laws, thermodynamic restrictions, energy density functions, and kinetic prescriptions needed to complete the theory. Section 4 consolidates the main elements of the theory and offers comparisons with dislocation-based plasticity models from the literature. A discussion of potential applications follows in the closing remarks, with a simple example given in Appendix A illustrating how the framework can facilitate description of the formation of cellular substructures observed in FCC metals at low homologous temperatures and large strains.

The following notation is used. Vector and tensor quantities are typically represented with boldface type, while scalars and individual components of vectors and tensors are written in italics. The index notation is often invoked for clarity, following the Einstein summation convention and distinguishing between covariant (subscript) and contravariant (superscript) components, unless noted otherwise. Current configuration indices are written in lower case Latin, reference configuration indices in upper case Latin, and intermediate configuration indices are written using Greek symbols. Juxtaposition implies summation over two repeated adjacent indices (e.g., $(\mathbf{AB})_a^{\cdot b} = A_{ac}B^{cb}$). The dot (scalar) product of vectors is represented by the symbol "$\bullet$" (e.g., $\mathbf{a} \bullet \mathbf{b} = a^a g_{ab} b^b$, with g_{ab} components of the metric tensor). Angled brackets denote a dual (scalar) product (e.g., for second-rank tensors, $\langle \mathbf{A},\mathbf{B} \rangle = \mathrm{tr}(\mathbf{AB}) = A_{ab}B^{ba}$, and for contra-covector pairs, $\langle \boldsymbol{\alpha},\mathbf{b} \rangle = \alpha_a b^a$). The colon denotes contraction over repeated pairs of indices (e.g., $\mathbf{A}:\boldsymbol{B} = \mathrm{tr}(\mathbf{A}^{\mathrm{T}}\mathbf{B}) = A_{ab}B^{ab}$ and $\mathbf{C}:\boldsymbol{A} = C^{abcd}A_{cd}$). The symbol "$\otimes$" represents the tensor (outer) product (e.g., $(\mathbf{a}\otimes\mathbf{b})^{ab} = a^a b^b$). Superposed -1, T, and "$\bullet$" denote inverse, transpose, and material time derivative operations, respectively. Additional notation is clarified later as it appears in the text.

2. Kinematics

Consider a crystalline volume element cut from a single crystal (though perhaps originally embedded within a polycrystal) and containing one or more lattice discontinuities (i.e., dislocation and/or disclination defects), as shown in Fig. 3. We invoke the following notation for configurations of volume elements: $v_0 \equiv b_0 \subset B_0$, $\tilde{v} \equiv \tilde{b} \subset \tilde{B}$, and $v \equiv b \subset B$, where global reference, intermediate, and current configurations of the entire macroscopic body are labeled B_0, $\tilde{B}$, and B, respectively. Typical dimensions of the referential volume v_0 are assumed to adhere to the following inequalities:

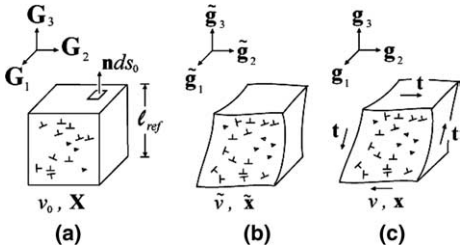

Fig. 3. Crystal volume element with defects: (a) reference configuration b_0, (b) unloaded intermediate configuration $\tilde{b}$, and (c) current configuration b.

$$a_0 \ll \ell_{\text{ref}} \leqslant L_{\text{G}}, \tag{1}$$

where $\ell_{\text{ref}} \equiv \sqrt[3]{v_0}$ is the scalar effective length of an edge of the reference volume element (Fig. 3(a)), and a_0 and L_{G} are the lattice parameter and average grain diameter, respectively. Taking $a_0 \approx 10^{-10}$ m and $L_{\text{G}} \approx 10^{-5}$ m–10^{-3} m as representative of engineering metals, we assume $\ell_{\text{ref}} \approx 10^{-8}$ m–10^{-4} m to satisfy Eq. (1). In Fig. 3 the sizes of the defects (e.g., Burgers vectors) relative to the size of the volume element are exaggerated for clarity of presentation. It is noted that we do not require the referential volume to constitute a statistically representative volume element in the sense of Hill (1972). Low defect densities are admissible. Dislocations are represented by the symbol $\perp$, and disclinations by the symbol $\triangleright$.

The three configurations of the volume element shown in Fig. 3 are defined as follows. The reference configuration volume v_0 is the crystal lattice as it existed prior to application of applied external forces (typically, and rather arbitrarily, at an initial time), such that it is free of traction along the external boundary s_0. The current configuration volume v is the deformed crystal lattice, with non-vanishing traction vector $\mathbf{t}$ per unit current area applied on its external boundary. The defects present in v_0 may slip over a finite distance as a result of the applied loading and may exit the volume element in the current configuration, and additional defects may enter the volume element during the history of loading. The intermediate configuration volume $\tilde{v}$ is achieved by unloading the current volume v by an inverse elastic deformation field $\mathbf{F}^{\mathbf{e}-1}$ associated with traction removal from the surface of the volume, as will be defined more precisely later. We remark that here $\tilde{v}$ is not necessarily the usual intermediate configuration of multiplicative finite elastoplasticity (cf. Lee and Liu, 1967; Asaro, 1983). The local deformation gradient $\mathbf{f}$ for material points with local coordinates X^A *within* the volume element v_0 is defined as the tangent mapping between reference and spatial configurations, i.e.,

$$\mathbf{f} \equiv T\boldsymbol{\phi}_X = \frac{\partial \phi^a}{\partial X^A}\mathbf{g}_a \otimes \mathbf{G}^A = x^a_{,A}\mathbf{g}_a \otimes \mathbf{G}^A, \tag{2}$$

where $\mathbf{g}_a$ and $\mathbf{G}^A$ are basis vectors and covectors assigned to the current and reference states, respectively, and $x^a = \varphi^a(X^A,t)$ away from displacement discontinuities. We note that $\mathbf{f}$ cannot be defined by Eq. (2) in locations in the immediate vicinity of slip planes over which dislocations have passed, for example, where the lattice

deformation is discontinuous. In other words, it is a discontinuous, anholonomic mapping in such locations (cf. Clayton et al., 2004b).

The total deformation gradient $\mathbf{F}$ for the crystal element is specified by the motion of its external boundary, assuming *homogeneous* basis vectors in the reference and current configurations for simplicity, i.e.,

$$\mathbf{F} \equiv \left[\frac{1}{v_0}\int_{s_0} x^a n_A \, \mathrm{d}s_0\right] \mathbf{g}_a \otimes \mathbf{G}^A = F^a_{\ A}\mathbf{g}_a \otimes \mathbf{G}^A, \tag{3}$$

with $\mathbf{n}\,\mathrm{d}s_0$ an oriented reference area element, as shown in Fig. 3. When a defect line crosses the element's boundary in the current state, the coordinates x^a will be multi-valued functions of X^A. In such cases we take for the contribution to (3) an average of the contributions of the coordinates x^{a+} and x^{a-} on opposite faces of the discontinuity at the boundary, i.e., $(2v_0)^{-1}\int_{s_0}(x^{a+}+x^{a-})n_A \, \mathrm{d}s_0$. Notice that when the local deformation field is purely elastic, meaning no defect generation or motion occurs between reference and current states, x^a are continuous, single-valued, and differentiable functions of X^A, and Eq. (3) reduces to

$$F^a_{\ A} = \frac{1}{v_0}\int_{s_0} \frac{\partial x^a}{\partial X^A}\,\mathrm{d}v_0 = \frac{1}{v_0}\int_{s_0} f^a_{\ A}\,\mathrm{d}v_0 \tag{4}$$

upon invocation of the generalized Gauss's theorem (Hill, 1972; also see derivation in Clayton and McDowell, 2003).

We define at the scale of the volume element a *recoverable elastic deformation gradient* $\mathbf{F^e} = \mathbf{V^e}\mathbf{R^e}$. The elastic stretch $\mathbf{V^e}$ is associated with the average externally applied stress acting on the element and is determined explicitly from (Clayton and McDowell, 2003)

$$\mathbf{V^e} = \left(\int_{s_0} \mathbf{x}\otimes\mathbf{n}\,\mathrm{d}s_0\right)\left(\int_{s_0}\hat{\mathbf{x}}\otimes\mathbf{n}\,\mathrm{d}s_0\right)^{-1}, \tag{5}$$

where $\hat{\mathbf{x}}$ are the local coordinates of the external boundary of the element corresponding to a specially defined, second traction-free intermediate configuration $\hat{b}$, i.e., with $\hat{\mathbf{t}} = \mathbf{0}$, as shown in Fig. 4. Configuration $\hat{b}$ arises from instantaneous removal of traction along the boundary, constrained such that rotation of the volume element, $\mathbf{R^{e-1}}$, does not occur. The unloading procedure is assumed instantaneous – to avoid viscous inelasticity upon load removal – with inertial effects neglected (Kratochvíl, 1971; Clayton and McDowell, 2003). Disclinations and dislocations within the volume element are locked in during this hypothetical process, with no defect motion or generation/annihilation permitted during unloading. Correspondingly, the defect populations in Figs. 3(b) and (c) are identical apart from the net elastic unloading and rigid body motion of the volume element. Since lattice defects are not introduced during unloading, $\mathbf{F^e}$ (or its inverse) does not alter the holonomicity (or lack thereof) of the material *within* the volume element, at the microscale. However, since the deformation achieved upon unloading may not be compatible across neighboring volume elements, $\mathbf{F^e}$ is generally anholonomic (i.e., incompatible) at the macroscale, in this case defined as corresponding to length scales significantly larger than that of the volume element shown in Fig. 3. In other words, when traction is

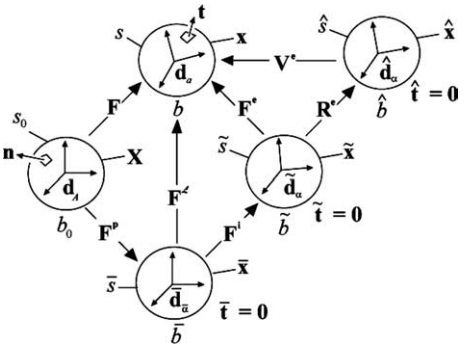

Fig. 4. Configurations and director vectors.

removed from the volume of the element, its boundary may undergo deformation that is compatible or incompatible with neighboring elements, with the degree of incompatibility depending upon the scale of volume considered relative to the distribution of defects contained within the volume. The elastic rotation tensor $\mathbf{R}^{\mathbf{e}}$ is determined such that each member of a triad of lattice director vectors assigned to the centroid of the crystal element deforms between configurations $\tilde{b}$ and b as

$$\mathbf{d}_a = \left(F^{e-1}\right)^{\alpha}_{.a}\tilde{\mathbf{d}}_{\alpha}, \tag{6}$$

with $(a, \alpha = 1, 2, 3)$. As depicted in Fig. 4, the director vectors in the current (b) and intermediate ($\tilde{b}$) configurations are labeled with Latin and Greek subscripts as $\mathbf{d}_a$ and $\tilde{\mathbf{d}}_{\alpha}$, respectively. Notice that these directors map between configurations in an analogous fashion to components of the "slip plane normal vectors" of conventional crystal plasticity theory (Asaro, 1983), and that $\mathbf{R}^{\mathbf{e}}$ is assumed to encompass any rigid body rotations of the entire (poly)crystal in global configuration B. Furthermore, when temperature changes occur, $\mathbf{F}^{\mathbf{e}}$ is assumed to capture the net thermal expansion or contraction of the volume element and the corresponding change in the lattice directors, most typically assumed in practice to be an isotropic deformation mode in engineering metals with cubic crystalline structure, though possibly anisotropic in non-cubic lattices (cf. Nye, 1957). In this context, the volume element in thermoelastically unloaded configuration $\tilde{b}$ is of uniform reference temperature and null average stress, and $\mathbf{F}^{\mathbf{e}}$ is referred to as the *recoverable thermoelastic deformation gradient*. The *total lattice deformation gradient*, introduced as $\mathbf{F}^{\mathscr{L}}$ in Fig. 4, is discussed in detail later in the text.

We next introduce the *average plastic deformation gradient* for the volume element, written here as $\mathbf{F}^{\mathbf{p}}$. As demonstrated by Teodosiu (1969), Rice (1971), and Ortiz and Repetto (1999), the discontinuous plastic deformation gradient in the vicinity of a single moving dislocation may be estimated in terms of the Burgers vector and slip plane geometry. When multiple mobile defects are considered, the time rate of plastic deformation over some finite volume (e.g., that of Fig. 3) may be characterized in terms of the defect fluxes, i.e.,

$$\bar{\mathbf{L}}^{\mathbf{p}} \equiv \dot{\bar{\mathbf{F}}}^{\mathbf{p}}\bar{\mathbf{F}}^{\mathbf{p}-1} = \left(\sum_j \bar{\boldsymbol{\alpha}}_t^j \otimes \dot{\bar{\boldsymbol{\xi}}}_+^j + \sum_k \kappa^k r^k \bar{\boldsymbol{\theta}}_t^k \otimes \dot{\bar{\boldsymbol{\zeta}}}_+^k\right) : \bar{\boldsymbol{\varepsilon}}, \tag{7}$$

with κ^k a scalar geometry factor (Li and Gilman, 1970) and $\bar{\boldsymbol{\varepsilon}}$ the rank three covariant permutation tensor. Generally hereafter, we use the overbar notation to refer to quantities framed in configuration $\bar{b}$ of Fig. 4. In Eq. (7), summation is applied over j populations of *straight* dislocation lines, each with velocity vector $\dot{\bar{\boldsymbol{\xi}}}_+^j$, and k populations of *straight* disclination lines, each with velocity vector $\dot{\bar{\boldsymbol{\zeta}}}_+^k$ and effective disclination radius r^k. The *total* (as opposed to *net*) dislocation and disclination density tensors introduced in (7) are defined as

$$\bar{\boldsymbol{\alpha}}_t^j \equiv \left(\bar{\rho}_+^j + \bar{\rho}_-^j\right)\bar{\mathbf{b}}_+^j \otimes \bar{\boldsymbol{\xi}}^j, \quad \bar{\boldsymbol{\theta}}_t^k \equiv \left(\bar{\eta}_+^k + \bar{\eta}_-^k\right)\bar{\boldsymbol{\omega}}_+^k \otimes \bar{\boldsymbol{\zeta}}^k, \tag{8}$$

with $\bar{\rho}_+^j$ and $\bar{\rho}_-^j$ the densities (line length per unit volume) of positively and negatively signed dislocations, where, for each value of j, the positive and negative dislocations share the same tangent line $\bar{\boldsymbol{\xi}}^j$ but oppositely oriented Burgers vectors $\bar{\mathbf{b}}_+^j = -\bar{\mathbf{b}}_-^j$ and velocities $\dot{\bar{\boldsymbol{\xi}}}_+^j = -\dot{\bar{\boldsymbol{\xi}}}_-^j$. Analogously, $\bar{\eta}_+^k$ and $\bar{\eta}_-^k$ are densities (line length per unit volume) of signed disclinations with tangent lines $\bar{\boldsymbol{\zeta}}^k$ and Frank vectors $\bar{\boldsymbol{\omega}}_+^k = -\bar{\boldsymbol{\omega}}_-^k$. Eq. (7) extends previous works of Teodosiu (1969), Lardner (1974), and Werne and Kelly (1978) to include disclination line contributions, following the paper by Li and Gilman (1970) on disclinations in polymers. Similar expressions could be formulated to include curved defect lines (cf. Teodosiu, 1969; Das et al., 1973), though these tend to be somewhat more complex as the tangent vectors of the defects are no longer spatially constant. For example, Teodosiu (1969) derived an expression for the velocity gradient contribution from a mobile density of strictly circular dislocation loops. The discrete approximation of (7) and (8) may be acceptable given that contemporary 3D dislocation dynamics models often piecewise-linearize curved dislocation segments (cf. Zbib et al., 1998).

Eqs. (7) and (8) have been introduced for illustrative purposes, to show how moving discrete crystal defects contribute to the time rate of change of $\mathbf{F}^{\mathbf{p}}$. Alternatively, we often find it more convenient to write Eq. (7) from the perspective of crystal plasticity kinematics, i.e.,

$$\bar{\mathbf{L}}^{\mathbf{p}} = \sum_i \dot{\gamma}^i \bar{\mathbf{s}}^i \otimes \bar{\mathbf{m}}^i + \bar{\mathbf{L}}_{\mathbf{v}}^{\mathbf{p}}, \tag{9}$$

where summation runs over i slip systems, each with shearing rate $\dot{\gamma}^i$, contravariant direction vector $\bar{\mathbf{s}}^i$, and plane normal covariant vector $\bar{\mathbf{m}}^i$. The term $\bar{\mathbf{L}}_{\mathbf{v}}^{\mathbf{p}}$ includes defect motions not readily describable in terms of slip or pseudo-slip, for example nonconservative plastic flow stemming from dislocation climb and certain motions of disclination tangent lines and/or axes of rotation accompanied by vacancy formation (Das et al., 1973). Shearing rates on each system may be expressed as

$$\dot{\gamma}^i = \bar{\rho}^i b v^i + \bar{\eta}^i \kappa r \omega z^i + \vartheta^i\left(\dot{\bar{\rho}}^i, \dot{\bar{\eta}}^i\right), \tag{10}$$

with $\bar{\rho}^i = \bar{\rho}_+^i + \bar{\rho}_-^i$ the *total* (as opposed to *net*) mobile dislocation line density, b the magnitude of the Burgers vector, v^i the signed mean scalar dislocation velocity,

$\bar{\eta}^i = \bar{\eta}^i_+ + \bar{\eta}^i_-$ the total mobile disclination density, ω the magnitude of a typical Frank vector, κ and r denoting a geometric factor and effective disclination radius both assumed identical over all slip systems for simplicity (this assumption can be relaxed to address a distribution of partial disclination dipoles), and z^i a signed mean scalar velocity of disclination lines moving on slip system i, in direction $\bar{\mathbf{s}}^i$. The first term in (10) follows from Orowan (1940), the second from Li and Gilman (1970). Contributions of time rates of generation and annihilation of mobile defect densities to the slip rates are embodied by the functions ϑ^i (cf. Pęcherski, 1983), which may additionally be extended to incorporate dislocation flux through boundaries of finite volumes (including effects of time rates of geometrically necessary dislocation densities), as suggested by Arsenlis et al. (2004). Velocities are assumed positive for defects moving in the slip direction $\bar{\mathbf{s}}^i$ and negative for those moving in the direction $-\bar{\mathbf{s}}^i$. The plastic deformation gradient $\mathbf{F^p}$ is assumed to leave the lattice director vectors unperturbed; as shown in Fig. 4, $\mathbf{d}_A$ and $\bar{\mathbf{d}}_{\bar{z}}$ are identical when represented in a consistent global coordinate system. Notice also that $\mathbf{F^p}$ is isochoric when $\bar{\mathbf{L}}^{\mathbf{p}}_{\mathbf{v}} = \mathbf{0}$ and $\bar{\mathbf{s}}^i$ and $\bar{\mathbf{m}}^i$ are orthogonal, i.e.,

$$\dot{J}^p = J^p \mathrm{tr}\left(\bar{\mathbf{L}}^{\mathbf{p}}\right) = J^p \sum_i \dot{\gamma}^i \langle \bar{\mathbf{s}}^i, \bar{\mathbf{m}}^i \rangle = 0, \tag{11}$$

where J^p is the Jacobian determinant of $\mathbf{F^p}$ and tr denotes the trace operation. We remark that the relative contribution of each of $\bar{\rho}^i$ and $\bar{\eta}^i$ to the plastic velocity gradient in (9) is set forth implicitly by the choice of flow rule for $\dot{\gamma}^i$ (see later Eq. (57)), formulation of which may be guided by heuristic kinetics principles such as maximal dissipation. Alternatively, one may approach the flow rule by capturing characteristics of dislocation and disclination driving forces versus velocities, explicitly describing $\dot{\gamma}^i$ in (10).

Consider for a moment the usual multiplicative decomposition $\mathbf{F} = \mathbf{F^e F^p}$ (Bilby et al., 1957; Kröner, 1960; Lee and Liu, 1967) in the context of our volume averaging framework. We have assumed that the entire deformation in fictitious configuration $\bar{b}$ is caused by the time-dependent generation and motion of displacement discontinuities (dislocations and disclinations) integrated over the activated slip planes, via the definitions of $\bar{\mathbf{L}}^{\mathbf{p}}$ in Eqs. (7) and (9). Neglected in the typical kinematic description $\mathbf{F} = \mathbf{F^e F^p}$, when applied to a crystalline volume of finite size, are the net effects of residual lattice deformation fields contained within the volume element. These local residual deformations are attributed to the local lattice strain fields in the vicinity of each defect line and may also include residual lattice deformations arising from thermal unloading from a heterogeneous temperature field. As a generalization of the two-term decomposition, we propose a three-term multiplicative decomposition for a crystal volume element (cf. Clayton and McDowell, 2003; Clayton et al., 2004a) consistent with Fig. 4, i.e.,

$$\mathbf{F} = \mathbf{F^e F^i F^p}, \tag{12}$$

with $\mathbf{F}$, $\mathbf{F^e}$, and $\mathbf{F^p}$ defined already, leaving

$$\mathbf{F^i} \equiv \mathbf{F^{e-1} F F^{p-1}}, \tag{13}$$

which may further decomposed as

$$\mathbf{F}^{\mathbf{i}} = \mathbf{V}^{\mathbf{i}}\mathbf{R}^{\mathbf{i}} = \mathbf{R}^{\mathbf{i}}\mathbf{U}^{\mathbf{i}}, \tag{14}$$

thus functioning as the net contribution to $\mathbf{F}$ of any residual elastic stretch ($\mathbf{V}^{\mathbf{i}}$, $\mathbf{U}^{\mathbf{i}}$) and rotation ($\mathbf{R}^{\mathbf{i}}$) of the crystal lattice remaining upon unloading by the applied stress. The residual lattice deformation arises from considering the (in)compatibility of microelastic lattice strains and rotations within the defect kinematic fields, as per the original concept of Bilby et al. (1955). The deformation (tangent) map $\mathbf{F}^{\mathbf{i}}$ of (13) is not necessarily a volume average, but rather an indicator of the net effects of local deformation heterogeneity on the total volume-averaged deformation gradient. Eqs. (7) and (9) regard the lattice as an aggregate of rigid "blocks" deforming by relative sliding on slip planes between the blocks. The local residual lattice deformation, whose net effects are embodied by $\mathbf{F}^{\mathbf{i}}$, is necessary to deform each block such that the aggregate fits together into a single continuous piece in configuration $\tilde{b}$ (Figs. 3 and 4), with the only displacement discontinuities within $\tilde{v}$ attributed to incompatibility in the immediate vicinity of the defect lines. Decomposition (12) was introduced by the present authors to describe elastoplastic polycrystals (Clayton and McDowell, 2003) and elastoplastic single crystals (Clayton et al., 2004a). It is introduced here from a slightly different standpoint, for (thermo)elastic single crystals containing a distribution of dislocation and disclination defects. We emphasize that description (12) is scale dependent, depending upon the size of the crystal volume element to which it is applied, and resolution dependent, depending upon the manner in which local kinematics within the volume element are resolved and accounted for in the homogenized description. Notice from Fig. 4 that $\mathbf{F}^{\mathbf{i}}$ affects the representation of the lattice directors, i.e.,

$$\bar{\mathbf{d}}_{\bar{\alpha}} = F^{i\alpha}_{\cdot\,\bar{\alpha}}\tilde{\mathbf{d}}_{\alpha}, \tag{15}$$

thereby accounting for slip system reorientation (see also later Eq. (63)) due to defects contained within the volume element in the unloaded state and also any cumulative director motion due to the disclination flux which, in contrast to the dislocation flux, generally induces a net lattice rotation (cf. Lardner, 1973; Pęcherski, 1983; and our later Eqs. (65)–(67)).

Fig. 5 conceptualizes the physics of Eq. (12) from the standpoint of (a) a Volterra process and (b) a corresponding lattice for a volume element containing a single edge dislocation. Notice how the displacement discontinuity in the wake of the dislocation (i.e., left side of the cylinder in Fig. 5(a)) is sealed by the residual lattice deformation gradient $\mathbf{F}^{\mathbf{i}}$. Prior to the application of $\mathbf{F}^{\mathbf{i}}$, for the body labeled $\bar{v}$ in Fig. 5, elastic strain fields are absent, and the plastic deformation gradient $\mathbf{F}^{\mathbf{p}}$ is completely defined in terms of the relative motion of the two halves of the lattice on opposite sides of the slip plane (dotted line in Fig. 5(b)). Note also that $\bar{v}$ is generally locally incompatible across the entire slip path, containing slip discontinuities but no lattice strains, and is free of internal residual stress fields. This is in contrast to $\tilde{v}$, which may contain internal residual stress and lattice strain fields but includes no discontinuities except for those in the immediate vicinity of individual defect lines contained within the volume.

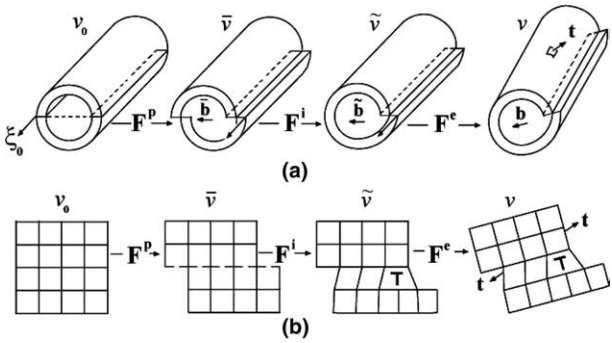

Fig. 5. Configurations of crystal element containing edge dislocation: (a) Volterra model and (b) lattice.

Please note that the particular sequence of deformation maps in (12) is chosen based on rational arguments. The plastic deformation term $\mathbf{F}^{\mathbf{p}}$ is the rightmost in our decomposition, as it leaves the lattice vectors unaltered (Fig. 4), permitting identification of configuration $\bar{b}$ of Fig. 4 with Mandel's (1973) isoclinic configuration. The residual deformation due to micro-heterogeneity in the presence of lattice defects, $\mathbf{F}^{\mathbf{i}}$, is placed second in our decomposition, as it affects the lattice directors via (15), yet is assumed unaffected by superposed rigid body motion or a change in spatial coordinate frame (Kratochvíl, 1972). Finally, the recoverable elastic deformation $\mathbf{F}^{\mathbf{e}}$ logically assumes the leftmost position, as the stretch $\mathbf{V}^{\mathbf{e}}$ is associated with unloading of the average traction acting on the volume element from the *current* state (Eq. (5)) and the rotation $\mathbf{R}^{\mathbf{e}}$ accounts for all lattice rotations not embodied in $\mathbf{F}^{\mathbf{i}}$, including net rigid body motions of the solid. The rotational components $\mathbf{R}^{\mathbf{i}}$ of $\mathbf{F}^{\mathbf{i}}$ and $\mathbf{R}^{\mathbf{p}}$ of $\mathbf{F}^{\mathbf{p}}$ are assumed to evolve independently of rigid body motions of the solid. Thus, under a change of spatial coordinates $\mathbf{x} \to \mathbf{\Omega x} + \mathbf{c}$, for which $\mathbf{\Omega}$ is a unimodular rotation satisfying $\mathbf{\Omega}^{\mathrm{T}} = \mathbf{\Omega}^{-1}$ and $\mathbf{c}$ is a spatially constant translation vector, the deformation maps transform according to $\mathbf{F} \to \mathbf{\Omega F}$, $\mathbf{F}^{\mathbf{e}} \to \mathbf{\Omega F}^{\mathbf{e}}$, $\mathbf{F}^{\mathbf{i}} \to \mathbf{F}^{\mathbf{i}}$, and $\mathbf{F}^{\mathbf{p}} \to \mathbf{F}^{\mathbf{p}}$.

We may also choose to introduce a fictitious local natural configuration ℓ free of all defect lines, slipped regions, and commensurate initial residual stresses, following Teodosiu (1969) and Rice (1971). Eq. (12) is then extended to $\mathscr{K} = \mathbf{F}\mathscr{K}_0 = \mathbf{F}^{\mathbf{e}}\mathbf{F}^{\mathbf{i}}\mathbf{F}^{\mathbf{p}}\mathscr{K}_0$ with $\mathscr{K}_0 : T\ell \to Tb_0$ the deformation gradient of the volume element due to the creation of defect lines, grain boundaries, etc. (and possible residual elastic lattice strains) present in the initial configuration v_0. For modeling the deformation of a structure from an engineering standpoint, knowledge of $\mathscr{K}_0$ and reconstruction of ℓ are not essential in our approach, since covariant components of the total deformation gradient $\mathbf{F}$ are referred to the actual state of the body at $t = 0$, denoted here by the local volume element v_0. Furthermore, changes in free energy are defined here with respect to the reference configuration or initial state, as opposed to the natural state. The residual stresses and energy commensurate with $\mathscr{K}_0$ are usually not considered explicitly in thermodynamic treatments of finite crystalline plasticity, even when the map $\mathscr{K}_0$ is introduced in the kinematics (Teodosiu, 1969; Rice,

1971; Teodosiu and Sidoroff, 1976; Hartley, 2003). Also, we mention that the aforementioned theories refer the covariant leg of the plastic deformation gradient to the generally anholonomic natural state, arriving at a decomposition $\mathbf{F} = \mathbf{F}^{\mathbf{e}}\mathbf{F}^{\mathbf{p}}\mathscr{K}_0^{-1}$. This contrasts with our model and those of Le and Stumpf (1996a) and Stumpf and Hoppe (1997) that refer the covariant components of the plastic deformation gradient to the (initial) reference configuration, which is holonomic to the current configuration. The first fundamental difference between our stress-free "natural configuration" ℓ and our stress-free "intermediate configuration" $\tilde{b}$ is this: the former is achieved via unloading each crystal element from the reference (i.e., initial) configuration, while the latter is realized via unloading each element from the spatial (i.e., current) configuration (Clayton et al., 2004b). The second difference is that while $\tilde{b}$ is achieved by external unloading of the local volume element, leaving this volume intact at the microscale (as conceptualized in Fig. 4 by applying $\mathbf{F}^{\mathbf{e}-1}$ to b, leading to configuration $\tilde{b}$ with conditions $\tilde{\mathbf{t}} = \mathbf{0}$), the natural configuration ℓ can only be achieved by cutting the local volume element v_0 into multiple pieces such that the initial residual stresses are relaxed at the scale of the individual pieces. Of course, when the initial configuration is a perfect lattice, such as in the left side of Fig. 5(b), free of initial elastic lattice deformation associated with defects, there is no distinction between what we call natural and reference configurations (i.e., ℓ and b_0 coincide) and $\mathscr{K}_0 = \mathbf{1}$. Although not pursued here, it is possible to assign the initial structure and lattice distortion fields corresponding to arbitrary initial defect topology as part of $\mathscr{K}_0$ if the resulting free energy and residual strain fields are of interest.

Others have proposed three-term multiplicative decompositions for continuum elastoplasticity exclusive of damage, although each within a slightly different context than the present work. Kratochvíl (1972) suggested the decomposition $\mathbf{F} = \mathbf{F}^{\mathbf{e}}\mathbf{F}^{\mathbf{i}}\mathbf{F}^{\mathbf{p}}$ for polycrystalline solids, with $\mathbf{F}^{\mathbf{e}}$ the recoverable elastic deformation, $\mathbf{F}^{\mathbf{p}}$ the viscoplastic deformation, and $\mathbf{F}^{\mathbf{i}}$ accounting for any other microstructural rearrangements – e.g., twinning and phase transitions – that influence the physical properties and hence, the specific free energy density. Horstemeyer (1995) and Horstemeyer and McDowell (1998) introduced the decomposition $\mathbf{F} = \mathbf{F}^{\mathbf{e}}\mathbf{F}^{\mathbf{i}}\mathbf{F}^{\mathbf{p}}$ for a single crystal, with $\mathbf{F}^{\mathbf{e}}$ and $\mathbf{F}^{\mathbf{p}}$ the usual elastic and plastic deformation gradient fields of crystal plasticity theory, and with $\mathbf{F}^{\mathbf{i}}$ representing time-dependent anelastic rearrangement of the crystalline lattice, associated with micro-residual stresses within the crystal, and possibly accounting for the lattice deformation accompanying grain subdivision. Also considering single crystal plasticity theory, Butler and McDowell (1998) proposed the decomposition $\mathbf{F} = \mathbf{F}^{\mathbf{e}}\mathbf{F}^{\mathbf{i}}\mathbf{F}^{\mathbf{p}}$, with $\mathbf{F}^{\mathbf{i}}$ directly associated with heterogeneous grain subdivision, distinct from the net contributions of dislocation glide embodied in $\mathbf{F}^{\mathbf{p}}$. Lion (2000) introduced a decomposition $\mathbf{F} = \mathbf{F}^{\mathbf{e}}\mathbf{F}^{\mathbf{i}}\mathbf{F}^{\mathbf{p}}$, with the macroscopic polycrystalline non-recoverable deformation decomposed into residual elastic ($\mathbf{F}^{\mathbf{i}}$) and plastic ($\mathbf{F}^{\mathbf{p}}$) parts. Bammann (2001) and Regueiro et al. (2002) suggested a similar three-term decomposition with $\mathbf{F}^{\mathbf{i}}$ the incompatible residual elastic deformation gradient and $\mathbf{F}^{\mathbf{e}}$ the superposed compatible elastic deformation due to the applied stress. Hartley (2003) suggested, from a discrete dislocation standpoint, the decomposition $\mathbf{F} = \mathbf{F}^{\mathbf{e}}\mathbf{F}^{\mathbf{i}}\mathbf{F}^{\mathbf{p}}\mathscr{K}_0^{-1}$ for a single- or polycrystalline volume element. In Hartley's model (2003), $\mathbf{F}^{\mathbf{e}}$ is a compatible recoverable elastic deformation gradient associated with

the traction acting on a representative volume of the material, and $\mathbf{F}^{\mathbf{i}}$ is further multiplicatively decomposed into terms representing residual elasticity due to dislocations contained within the volume element and incompatible elasticity due to sources of deformation outside the element (e.g., intergranular incompatibility).

Our deformation mapping $\mathbf{F}^{\mathbf{i}}$ includes effects arising from defects contained within the volume element at time t, residual thermoelastic strains, and internal boundaries and stacking faults left by moving defects such as partial dislocations and partial disclination dipoles. Lattice-preserving contributions from mobile defects that have traversed the volume prior to time t are embodied in the rate equations for $\mathbf{F}^{\mathbf{p}}$, (7)–(10). It should be noted that our Eq. (12) is a multiscale decomposition, with the meaning of each term dependent upon the specific scale (i.e., size of (poly)crystalline volume element) to which it is applied, as discussed in Clayton and McDowell (2003). If enforced over a relatively homogeneously deforming region encompassing a statistically large number of grains, or a region encompassing a single crystal containing a random distribution of defects for which there is no net Burgers vector (i.e., statistically stored defects only), one would expect $\mathbf{F}^{\mathbf{i}} \to \mathbf{1}$ and $\mathbf{F}^{\mathbf{e}}$ to be a holonomic deformation field within this region, making $\bar{b}$ a compatible configuration. On the other hand, when (12) is applied to describe a single crystal or polycrystal subjected to nonuniform deformation (i.e., strain gradients), the corresponding volume element will generally exhibit lattice curvature due to geometrically necessary defects, $\mathbf{F}^{\mathbf{i}}$ will not reduce to the identity mapping due to non-negligible net effects of residual lattice deformation, and $\mathbf{F}^{\mathbf{e}}$ will be anholonomic as a result of the heterogeneous stress state existing across neighboring elements. We also remark that continuum finite element simulations (Clayton and McDowell, 2003; Clayton et al., 2004a) suggest that the magnitude of the stretch $\mathbf{V}^{\mathbf{i}}$ of Eq. (14) remains small relative to that of the total applied stretch in isothermally deforming single crystals containing low-angle subgrain boundaries.

The deformation of the lattice director vectors between configurations $\bar{b}$ and b, as depicted in Fig. 4, is dictated by the total lattice deformation $\mathbf{F}^{\mathscr{L}} \equiv \mathbf{F}^{\mathbf{e}}\mathbf{F}^{\mathbf{i}}$:

$$\mathbf{d}_a = \left(F^{\mathscr{L}-1}\right)_{.a}^{\bar{\alpha}} \bar{\mathbf{d}}_{\bar{\alpha}}. \tag{16}$$

Assuming that the directors in configuration $\bar{b}$ are orthonormal, and assigning an external Cartesian coordinate system to the anholonomic space $\bar{b}$ with corresponding metric tensor

$$\bar{\mathbf{d}}_{\bar{\alpha}} \bullet \bar{\mathbf{d}}_{\bar{\beta}} = \bar{g}_{\bar{\alpha}\bar{\beta}} = \delta_{\bar{\alpha}\bar{\beta}}, \tag{17}$$

we define a metric $\mathbf{C}^{\mathscr{L}}$ in the spatial configuration associated with the total director strain:

$$C^{\mathscr{L}}_{ab} \equiv \mathbf{d}_a \bullet \mathbf{d}_b = F^{\mathscr{L}-1\bar{\alpha}}_{.a} F^{\mathscr{L}-1\bar{\beta}}_{.b} \bar{\mathbf{d}}_{\bar{\alpha}} \bullet \bar{\mathbf{d}}_{\bar{\beta}} = F^{\mathscr{L}-1\bar{\alpha}}_{.a} \delta_{\bar{\alpha}\bar{\beta}} F^{\mathscr{L}-1\bar{\beta}}_{.b}. \tag{18}$$

Also introduced are coefficients of a linear (i.e., affine) connection $\boldsymbol{\Gamma}$ (cf. Eisenhart, 1926; Schouten, 1954; Wang and Truesdell, 1973) describing the absolute change of the director vector field in the current configuration in terms of the covariant derivative ∇, i.e.,

$$\nabla_b \mathbf{d}_a = \mathbf{d}_{a,b} - \Gamma^{\cdot\cdot c}_{ba}\mathbf{d}_c, \tag{19}$$

with the subscripted comma denoting partial differentiation with respect to current coordinates $\mathbf{x}$. The connection coefficients are defined by (Minagawa, 1979, 1981)

$$\Gamma^{\cdot\cdot a}_{cb} \equiv F^{\mathscr{L}a}_{\cdot\bar{\alpha}} F^{\mathscr{L}-1\bar{\alpha}}_{\cdot b,c} + Q^{\cdot\cdot a}_{cb} = \bar{\Gamma}^{\cdot\cdot a}_{cb} + Q^{\cdot\cdot a}_{cb}, \tag{20}$$

where $\bar{\Gamma}^{\cdot\cdot a}_{cb} \equiv F^{\mathscr{L}a}_{\cdot\bar{\alpha}} F^{\mathscr{L}-1\bar{\alpha}}_{\cdot b,c} = -F^{\mathscr{L}a}_{\cdot\bar{\alpha},c} F^{\mathscr{L}-1\bar{\alpha}}_{\cdot b}$ are coefficients of the so-called "crystal connection" of non-Riemannian dislocation theories (Bilby et al., 1955; Noll, 1967; Le and Stumpf, 1996b), and $Q^{\cdot\cdot a}_{cb}$ are additional micropolar degrees-of-freedom representing contributions of distributed disclinations to the spatial gradients of the lattice director field. When disclinations are absent and the lattice directors are spatially uniform in configuration $\bar{b}$, the expression for parallel transport $\mathbf{d}_{a,b} = \bar{\Gamma}^{\cdot\cdot c}_{ba}\mathbf{d}_c$ describes, to first order, the deformed lattice. Upon assuming that $\nabla_b \mathbf{d}_a = 0$ (Minagawa, 1981), the connection (20) allows one to interpolate for the directions and magnitudes of the lattice directors between centroids of neighboring crystal volume elements. For example, in the trivial case when $\Gamma^{\cdot\cdot a}_{cb} = 0$, the lattice directors are spatially constant. The crystal connection ($\bar{\mathbf{\Gamma}}$) component of (20) accounts for effects of first-order spatial gradients of (the inverse of) $\mathbf{F}^{\mathscr{L}}$, while the variable $\mathbf{Q}$ of (20) accounts for the additional spatial variations of lattice directors not captured by the first spatial gradient of $\mathbf{F}^{\mathscr{L}}$. The *average* continuum deformation of the director vectors located at the volume element's centroid is determined by $\mathbf{F}^{\mathscr{L}}$, as indicated by Eq. (16). Lattice stretch and rotation *gradients* (e.g., at the scale of subgrain cells and cell blocks) in the current configuration are represented by the coefficients (20). Note that unlike the deformation gradient, $\mathbf{\Gamma}$ is not a two-point tensor or configurational mapping, but rather a spatial operator. The covariant components of $\mathbf{Q}$ are assigned the following anti-symmetry property (recall that we use italic font for individual components of non-scalar entities such as $\mathbf{Q}$)

$$Q_{cba} \equiv Q^{\cdot\cdot d}_{cb} C^{\mathscr{L}}_{da} = -Q_{cab} = Q_{c[ba]}, \tag{21}$$

with bracketed indices anti-symmetrized, i.e., $2Q_{c[ba]} = Q_{cba} - Q_{cab}$. Quantities Q_{cba} and $Q^{\cdot\cdot a}_{cb}$ are effectively equivalent rotation measures only when lattice strains are negligible, i.e., when $C^{\mathscr{L}}_{da} \approx \delta_{da}$. From (21), the connection is metric, since the covariant derivative of $\mathbf{C}^{\mathscr{L}}$ vanishes:

$$\nabla_c C^{\mathscr{L}}_{ab} = \underbrace{C^{\mathscr{L}}_{ab,c} - \bar{\Gamma}^{\cdot\cdot d}_{ca} C^{\mathscr{L}}_{db} - \bar{\Gamma}^{\cdot\cdot d}_{cb} C^{\mathscr{L}}_{ad}}_{=0} - Q^{\cdot\cdot d}_{ca} C^{\mathscr{L}}_{db} - Q^{\cdot\cdot d}_{cb} C^{\mathscr{L}}_{ad} = -2Q_{c(ab)} = 0, \tag{22}$$

where parentheses denote symmetrization, e.g., $2Q_{c(ba)} = Q_{cba} + Q_{cab}$. Components of the torsion tensor $\mathbf{T}$ of the connection $\mathbf{\Gamma}$ are given by

$$T^{\cdot\cdot a}_{cb} \equiv \Gamma^{\cdot\cdot a}_{cb} - \Gamma^{\cdot\cdot a}_{bc} = \bar{T}^{\cdot\cdot a}_{cb} + 2Q^{\cdot\cdot a}_{[cb]}, \tag{23}$$

where $\bar{T}^{\cdot\cdot a}_{cb}$ is the torsion of the crystal connection, often associated with the density of geometrically necessary dislocations when disclinations are absent (Bilby et al., 1955; Kröner, 1960; Noll, 1967). The components of the Riemann–Christoffel curvature tensor $R^{\cdot\cdot a}_{bcd}$ formed from the connection coefficients $\Gamma^{\cdot\cdot a}_{cb}$ are defined as (Schouten, 1954; Marsden and Hughes, 1983)

$$R^{\cdot\cdot a}_{bcd} \equiv \Gamma^{\cdot\cdot a}_{db,c} - \Gamma^{\cdot\cdot a}_{cb,d} + \Gamma^{\cdot\cdot a}_{ce}\Gamma^{\cdot\cdot e}_{db} - \Gamma^{\cdot\cdot a}_{de}\Gamma^{\cdot\cdot e}_{cb}, \tag{24}$$

which, because $\Gamma^{\cdot\cdot a}_{cb} = \bar{\Gamma}^{\cdot\cdot a}_{cb} + Q^{\cdot\cdot a}_{cb}$, we are able to rewrite as

$$R^{\cdot\cdot a}_{bcd} = \underbrace{\bar{R}^{\cdot\cdot a}_{bcd}}_{=0} + 2\nabla_{[c}Q^{b\cdot\cdot a}_{d]} + Q^{\cdot\cdot a}_{ce}Q^{\cdot\cdot e}_{db} - Q^{\cdot\cdot a}_{de}Q^{\cdot\cdot e}_{cb} + T^{\cdot\cdot e}_{cd}Q^{\cdot\cdot a}_{eb}, \tag{25}$$

where the curvature from the crystal connection, $\bar{R}^{\cdot\cdot a}_{bcd}$, vanishes identically since $\bar{\boldsymbol{\Gamma}}$ is integrable (cf. Le and Stumpf, 1996b). Using (21), we can express the fully covariant rendition of the curvature tensor, $R_{abcd} \equiv C^{\mathscr{L}}_{af}R^{\cdot\cdot\cdot f}_{bcd}$, as (Minagawa, 1979)

$$R_{[ab]cd} = 2\nabla_{[c}Q_{d][ba]} + T^{\cdot\cdot e}_{cd}Q_{e[ba]}, \quad R_{(ab)cd} = 2\nabla_{[c}Q_{d](ab)} + T^{\cdot\cdot e}_{cd}Q_{e(ab)} = 0. \tag{26}$$

Thus from (24) and (26), $R_{abcd} = R_{[ab][cd]}$, and $\mathbf{R}$ vanishes completely when $\mathbf{Q} = \mathbf{0}$.

Consider a Burgers circuit c in the current configuration, enclosing area a comprised of oriented differential elements $\mathbf{n}\,\mathrm{d}a$. A total Burgers vector accounting for the incompatibility induced by the torsion and curvature tensors may be written as (Lardner, 1973; Minagawa, 1979)

$$B^a \equiv \varepsilon^{dbc}\int_a \left(T^{\cdot\cdot a}_{bc} - R^{\cdot\cdot\cdot a}_{ecb}x^e\right)n_d\,\mathrm{d}a = B^a_T + B^a_R, \tag{27}$$

where $2B^a_T \equiv \varepsilon^{dbc}\int_a T^{\cdot\cdot a}_{bc}n_d\,\mathrm{d}a$ describes the closure failure of c and $2B^a_R \equiv \varepsilon^{bdc}\int_a R^{\cdot\cdot\cdot a}_{ecb}x^e n_d\,\mathrm{d}a$ measures the change in direction of position vector x^e upon parallel transport about c with respect to the connection $\boldsymbol{\Gamma}$. We can re-write (27) in terms of the second rank geometrically necessary dislocation tensor $\boldsymbol{\alpha}$ and second rank geometrically necessary disclination tensor $\boldsymbol{\theta}$, each referred to the current configuration b:

$$B^a = \int_a \left(\alpha^{ad} + C^{\mathscr{L}-1af}\varepsilon_{fgb}\theta^{gd}x^b\right)n_d\,\mathrm{d}a, \tag{28}$$

where

$$2\alpha^{ad} \equiv \varepsilon^{dbc}T^{\cdot\cdot a}_{bc}, \quad 4\theta^{gd} \equiv \varepsilon^{gba}\varepsilon^{dce}R_{abce}. \tag{29}$$

Fig. 6(a) illustrates the total Burgers vector $\mathbf{B} = \mathbf{B_T} + \mathbf{B_R}$ introduced in Eq. (27) in terms of parallel transport of a lattice director vector $\boldsymbol{d}_a$ about an incompatibility circuit c (Kondo, 1964). When viewed from the standpoint of a Volterra process

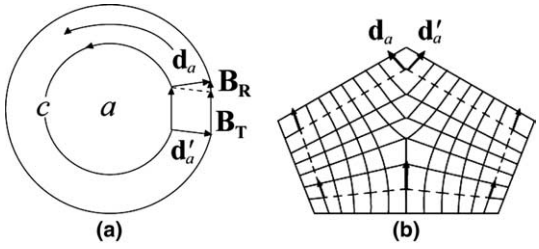

Fig. 6. Burgers vector with contributions from (a) dislocations ($\mathbf{B_T}$) and disclinations ($\mathbf{B_R}$), and (b) director vector rotation due to 60° wedge disclination.

(Fig. 1), one can imagine the body in Fig. 6(a) to consist of the superposition of a single edge dislocation (producing the incompatibility $\mathbf{B_T}$) and a single wedge disclination (producing the incompatibility $\mathbf{B_R}$). Fig. 6(b) shows the rotation of a director parallel-transported about a complete 60° wedge disclination in a hexagonal lattice (Lardner, 1974).

Notice that $\boldsymbol{\alpha}$ and $\boldsymbol{\theta}$ contain enough information to fully reconstruct $\mathbf{T}$ and $\mathbf{R}$, respectively, because of the skew-symmetry properties of these quantities:

$$T^{..a}_{cb} = T^{..a}_{[cb]} = \varepsilon_{cbd}\alpha^{ad}, \quad R_{abcd} = R_{[ab][cd]} = \varepsilon_{bae}\varepsilon_{cdf}\theta^{ef}. \tag{30}$$

The geometrically necessary defect density tensors of (29) are related to the summed contributions of discrete crystal defects as

$$\boldsymbol{\alpha} = \sum_j \rho^j \mathbf{b}^j \otimes \boldsymbol{\xi}^j, \quad \boldsymbol{\theta} = \sum_k \eta^k \boldsymbol{\omega}^k \otimes \boldsymbol{\zeta}^k, \tag{31}$$

with ρ^j, $\mathbf{b}^j$, and $\boldsymbol{\xi}^j$ the *net* scalar dislocation line density, Burgers vector, and unit tangent line, respectively, for dislocation population j, and with η^k, $\boldsymbol{\omega}^k$, and $\boldsymbol{\zeta}^k$ the *net* scalar disclination line density, Frank vector, and unit tangent line vector, respectively, for disclination population k. All quantities in (31) are referred to the spatial configuration b.

Notice that $\boldsymbol{\alpha}$ and $\boldsymbol{\theta}$ do not account for curved defect segments and combinations of defect lines that contribute no net Burgers vector or Frank vector. This becomes clear when we re-write (31) in terms of positively and negatively signed populations (Werne and Kelly, 1978):

$$\boldsymbol{\alpha} = \sum_j \left(\rho^j_+ - \rho^j_-\right)\mathbf{b}^j_+ \otimes \boldsymbol{\xi}^j, \quad \theta = \sum_k \left(\eta^k_+ - \eta^k_-\right)\boldsymbol{\omega}^k_+ \otimes \boldsymbol{\zeta}^k, \tag{32}$$

where $\mathbf{b}^j_+ = -\mathbf{b}^j_-$ and $\boldsymbol{\omega}^k_+ = -\boldsymbol{\omega}^k_-$. As discussed following (8), curved defect segments can be treated via piecewise linearization (Zbib et al., 1998; Zbib and De La Rubia, 2002) in order to address the distribution of line tangents of curved dislocation lines. We emphasize that the *total* mobile defect densities of (8) contribute to the plastic velocity gradient (7), while the *net* defect densities (both mobile and immobile) contribute to the equivalent incompatibility measures in (29), (31) and (32). Ashby (1970) introduced the concept of statistically stored dislocations to represent defects that accumulate under homogeneous plastic flow but do not contribute to net incompatibility. Later we appeal to this concept by introducing densities of statistically stored dislocations and statistically stored disclinations allowing us to quantify influences of differences between total cumulative defect densities and the geometrically necessary densities.

Linearized compatibility equations for the net defect density tensors of (29), (31) and (32) follow from identities of Bianchi and Schouten (cf. Schouten, 1954), expressed in Cartesian coordinates as

$$T^{..a}_{[bc,d]} = R^{...a}_{[bcd]} \rightarrow \left(C^{\mathscr{L}}\alpha\right)^{.b}_{a,b} = \varepsilon_{abc}\theta^{bc}, \quad R^{...a}_{b[cd,e]} = 0 \rightarrow \theta^{ab}_{,b} = 0. \tag{33}$$

In a small-strain formulation (i.e., additive elastoplastic strains and rotation gradients), De Wit (1981) inferred from equations analogous to (33) that disclinations

may act as sources/sinks for dislocations, and that disclination lines cannot end abruptly within a crystal. This linearization, while physically illustrative, is not essential in our general finite strain and rotation framework.

Complete pull-backs of $\boldsymbol{\alpha}$ and $\boldsymbol{\theta}$ to the intermediate configuration $\tilde{b}$ are written as follows:

$$\begin{aligned}\tilde{\alpha}^{\alpha\beta} &\equiv J^e F^{e-1\alpha}_{\ .a}\alpha^{ab}F^{e-1\beta}_{\ .b}\\ &= J^e F^{e-1\alpha}_{\ .a}\varepsilon^{bcd}F^{\mathscr{L}a}_{\ .\bar{\alpha}}F^{\mathscr{L}-1\bar{\alpha}}_{\ .d,c}F^{e-1\beta}_{\ .b} + J^e F^{e-1\alpha}_{\ .a}\varepsilon^{bdc}Q^{..a}_{[dc]}F^{e-1\beta}_{\ .b},\end{aligned} \tag{34}$$

$$\tilde{\theta}^{\alpha\beta} \equiv J^e F^{e-1\alpha}_{\ .a}\theta^{ab}F^{e-1\beta}_{\ .b} = \frac{1}{4}J^e F^{e-1\alpha}_{\ .a}\varepsilon^{adg}\varepsilon^{bce}R_{[gd][ce]}F^{e-1\beta}_{\ .b}, \tag{35}$$

with J^e the Jacobian determinant of $\mathbf{F}^e$. Variables $\tilde{\boldsymbol{\alpha}}$ and $\tilde{\boldsymbol{\theta}}$ may be regarded as "elastic" in the sense that they are derived completely from lattice kinematic quantities $\mathbf{F^e}$, $\mathbf{F^i}$, $\mathbf{Q}$ and/or spatial gradients of $\mathbf{F^e}$, $\mathbf{F^i}$, and $\mathbf{Q}$. On the other hand, the following "plastic" quantities are now introduced in the sense of push-forwards from the reference configuration:

$$\tilde{\alpha}_p^{\alpha\beta} \equiv -\tilde{J}^{-1}\tilde{F}^{\alpha}_{\ .A}\varepsilon^{BCD}F^{p\bar{\alpha}}_{D,C}F^{p-1A}_{\bar{\alpha}}\tilde{F}^{\beta}_{\ .B} - \tilde{J}^{-1}\tilde{F}^{\alpha}_{\ .A}\varepsilon^{BDC}\hat{Q}^{..A}_{[DC]}\tilde{F}^{\beta}_{\ .B}, \tag{36}$$

$$\tilde{\theta}_p^{\alpha\beta} \equiv -\tilde{J}^{-1}\tilde{F}^{\alpha}_{\ .A}\hat{\theta}^{AB}\tilde{F}^{\beta}_{\ .B} = -\frac{1}{4}\tilde{J}^{-1}\tilde{F}^{\alpha}_{\ .A}\varepsilon^{ADG}\varepsilon^{BCE}\hat{R}_{[GD][CE]}\tilde{F}^{\beta}_{\ .B}, \tag{37}$$

with $\tilde{F}^{\alpha}_{\ .A} \equiv F^{i\alpha}_{\bar{\alpha}}F^{p\bar{\alpha}}_{A}$ the residual deformation gradient and $\tilde{J}$ the Jacobian determinant of $\tilde{\mathbf{F}}$. By $\hat{\mathbf{Q}}$ and $\hat{\mathbf{R}}$ we denote, respectively, a generalized rank 3 inelastic micro-rotation variable and rank 4 curvature tensor on the reference coordinate frame such that the "total" defect densities $\tilde{\boldsymbol{\alpha}}_{\mathbf{T}}$ and $\tilde{\boldsymbol{\theta}}_{\mathbf{T}}$ vanish in the intermediate configuration, i.e.,

$$\tilde{\boldsymbol{\alpha}}_{\mathbf{T}} \equiv \tilde{\boldsymbol{\alpha}} + \tilde{\boldsymbol{\alpha}}_{\mathbf{p}} = \mathbf{0}, \quad \tilde{\boldsymbol{\theta}}_{\mathbf{T}} \equiv \tilde{\boldsymbol{\theta}} + \tilde{\boldsymbol{\theta}}_{\mathbf{p}} = \mathbf{0}. \tag{38}$$

Please note that $\hat{\mathbf{Q}}$ of (36) and $\hat{\mathbf{R}}$ of (37) are not constrained to be compatible with a linear connection defined on the reference frame, in contrast to $\mathbf{Q}$ of (34) and $\mathbf{R}$ of (35) which are compatible with the connection coefficients $\boldsymbol{\Gamma}$ of Eq. (20) in the current configuration. Equations given in (38) are equivalent to the additive relations of Eringen and Claus (1970) in the linearized limit. Also, when disclinations vanish, $\mathbf{Q} = \mathbf{0}$, $\tilde{\boldsymbol{\theta}} = \tilde{\boldsymbol{\theta}}_{\mathbf{p}} = \mathbf{0}$, and the first of (38) gives $J^e F^{e-1\alpha}_{\ .a}\varepsilon^{bcd}F^{\mathscr{L}a}_{\ .\bar{\alpha}}F^{\mathscr{L}-1\bar{\alpha}}_{\ .d,c}F^{e-1\beta}_{\ .b} = \tilde{J}^{-1}\tilde{F}^{\alpha}_{\ .A}\varepsilon^{BCD}F^{p\bar{\alpha}}_{D,C}F^{p-1A}_{\bar{\alpha}}\tilde{F}^{\beta}_{\ .B}$, following automatically from relations $\mathbf{F} = \mathbf{F^e}\mathbf{F^i}\mathbf{F^p} = \mathbf{F}^{\mathscr{L}}\mathbf{F^p}$ and $\oint_c \mathbf{F}^{\mathscr{L}-1}\,\mathrm{d}\mathbf{x} = \oint_C \mathbf{F^p}\,\mathrm{d}\mathbf{X}$ for current (reference) Burgers circuit c (C).

3. Balance laws, thermodynamics, and constitutive framework

The net nominal stress for the crystalline element illustrated in Fig. 3 is defined as

$$\mathbf{S} \equiv \frac{1}{v_0}\int_{s_0}\mathbf{X}\otimes\mathbf{t}_0\,\mathrm{d}s_0, \tag{39}$$

where $\mathbf{t}_0$ is the traction vector per unit reference area. Eq. (39) reduces to $v_0\mathbf{S} = \int_{v_0}\mathbf{s}\,\mathrm{d}v_0$, with $\mathbf{s}$ the local nominal stress *within* the volume element, only under quasi-static conditions and when discontinuities within the volume are traction-free (Nemat-Nasser, 1999). The net Cauchy stress is defined by

$$\boldsymbol{\Sigma}^{ab} \equiv J^{-1}F^{a}_{\ A}S^{Ab}, \tag{40}$$

with $J \equiv \det(\mathbf{F})\sqrt{g/G}$ the Jacobian determinant of the deformation gradient $\mathbf{F}$, and g and G determinants of metric tensors g_{ab} and G_{AB} associated, respectively, with spatial and reference coordinate systems shown in Fig. 3. Standard balances of mass, linear momentum, and angular momentum at the level of the volume element are now, respectively, asserted, i.e.,

$$\rho_0 = \rho J, \quad S^{Aa}_{\ \ |A} + \rho_0\hat{f}^{a} = \rho_0\ddot{x}^{a}, \quad F^{a}_{\ A}S^{Ab} = S^{Aa}F^{b}_{\ A}, \tag{41}$$

with ρ_0, ρ, and $\hat{f}^{a}$ the reference mass density, current mass density, and body force component per unit reference volume, respectively, and the vertical bar denoting covariant differentiation with respect to the reference coordinate system. From (40) and the last of (41), $\boldsymbol{\Sigma}^{ab} = \boldsymbol{\Sigma}^{(ab)}$. We add the caveat that one may choose to delve at this point into a polar or hyperstress theory (cf. Toupin, 1962; Garikipati, 2003) for which the Cauchy stress tensor is non-symmetric if dislocation spacings are on the order of the length scale of the volume element, or if the volume element has a strong net dislocation density resulting in local stress fluctuations that may translate into higher order moments of stress on the same order of magnitude as the average stress, Eq. (39). For simplicity we assume here that the volume element considered is large enough to permit us to neglect higher order stresses in the macroscopic momentum balances of (41), though we shall account explicitly for the net effects of heterogeneity of lattice deformation through inclusion of $\mathbf{F}^{\mathbf{i}}$ and the defect density tensors (representing lattice curvature) in the free energy function, microscopic momentum balances, and kinetics framework that follow.

Introducing the average internal energy per unit reference volume U_0, effective heat flux vector $\mathbf{q}$, and average heat generation per unit reference volume H_0, the local form of the balance of energy is written

$$\dot{U}_0 = S^{Aa}g_{ab}\dot{F}^{b}_{\ A} - q^{A}_{\ |A} + H_0, \tag{42}$$

where the quantities in (42) are averaged over a local volume element of size consistent with the preceding discussion accompanying (39). The entropy production and reduced dissipation inequalities are written in the reference frame as

$$\dot{N}_0 \geqslant \frac{H_0}{T} - \left(\frac{q^{A}}{T}\right)_{|A}, \quad S^{Aa}g_{ab}\dot{F}^{b}_{\ A} - \frac{1}{T}\left(q^{A}T_{|A}\right) \geqslant \dot{\psi}_0 + N_0\dot{T}, \tag{43}$$

with N_0 the entropy per unit reference volume and the Helmholtz free energy $\psi_0 \equiv U_0 - N_0T$. Thermodynamic restrictions (cf. Coleman and Noll, 1963; Coleman and Gurtin, 1967) can be deduced from inequalities (43), the second written in terms of two-point tensors $\mathbf{S}$ and $\mathbf{F}$ and the free energy per unit reference volume ψ_0. We find it useful to express (43) in terms of quantities with all components referred to

intermediate configuration $\tilde{b}$ of Fig. 3 (i.e., the reference state for instantaneous thermoelastic response – cf. Scheidler and Wright, 2001), which we view as the most convenient configuration for deducing thermodynamic restrictions and posing constitutive assumptions (see also Regueiro et al., 2002). After somewhat lengthy but standard manipulations (see Clayton et al., 2004a), the second of (43) can be written as

$$\tilde{L}^{\alpha}_{.\beta}\tilde{M}^{T\beta}_{.\alpha} - \tilde{\psi}\dot{\tilde{F}}^{\alpha}_{.A}\tilde{F}^{-1A}_{.\alpha} - \frac{1}{T}(\tilde{q}^{\alpha}T_{,\alpha}) \geqslant \dot{\tilde{\psi}} + \tilde{N}\dot{T}, \tag{44}$$

where $\tilde{L}^{\alpha}_{.\beta} \equiv F^{e-1\alpha}_{.a}\dot{F}^{a}_{.A}F^{-1A}_{.b}F^{eb}_{.\beta}$ is a velocity gradient, $\tilde{M}^{\alpha}_{.\beta} \equiv J^{e}F^{eT\alpha}_{.a}\Sigma^{ac}g_{cb}F^{e-Tb}_{.\beta}$ is the Mandel stress (Mandel, 1974), and the heat flux vector referred to $\tilde{b}$ is defined by $\tilde{q}^{\alpha} \equiv \tilde{J}^{-1}\tilde{F}^{\alpha}_{.A}q^{A}$, with the anholonomic temperature gradient $T_{,\alpha} \equiv T_{|A}\tilde{F}^{-1A}_{.\alpha}$. The free energy and entropy per unit volume in $\tilde{b}$ are found by $\tilde{\psi} = \tilde{J}^{-1}\psi_0$ and $\tilde{N} = \tilde{J}^{-1}N_0$, respectively.

We make the following general assumption regarding the dependency of the Helmholtz free energy function for the crystalline volume element, referred to configuration $\tilde{b}$ and neglecting the effects of temperature gradients *within* the element:

$$\tilde{\psi} = \tilde{\psi}\left(\tilde{\mathbf{C}}^{\mathbf{e}}, \mathbf{V}^{\mathbf{i}}, \tilde{\boldsymbol{\alpha}}, \tilde{\boldsymbol{\theta}}, \tilde{\varepsilon}_{\rho}, \tilde{\varepsilon}_{\eta}, T, \tilde{\mathbf{g}}\right) = \tilde{\psi}\left(\tilde{C}^{e}_{\alpha\beta}, V^{i\alpha}_{.\beta}, \tilde{\alpha}^{\alpha\beta}, \tilde{\theta}^{\alpha\beta}, \tilde{\varepsilon}_{\rho}, \tilde{\varepsilon}_{\eta}, T, \tilde{g}_{\alpha\beta}\right). \tag{45}$$

The covariant elastic strain tensor $\tilde{C}^{e}_{\alpha\beta} \equiv F^{ea}_{.\alpha}g_{ab}F^{eb}_{.\beta}$ is included to model the change of average elastic energy density with a change of external loads, a standard constitutive assumption in finite crystalline elastoplasticity theories (cf. Le et al., 1998). The left stretch tensor associated with $\mathbf{F}^{\mathbf{i}}$, denoted by $\mathbf{V}^{\mathbf{i}}$, is incorporated to reflect contributions to the free energy from residual microelasticity within the volume element, and may be non-negligible when the deformation within the volume element is heterogeneous (Clayton and McDowell, 2003). The elastic energies due to net lattice curvatures in the volume element induced by geometrically necessary dislocations and disclinations are reflected, respectively, by the inclusion of $\tilde{\boldsymbol{\alpha}}$ and $\tilde{\boldsymbol{\theta}}$, defined in (34) and (35). As a point of clarification, recall that the *total mobile* defect density tensors $\bar{\boldsymbol{\alpha}}^{j}_{t}$ and $\bar{\boldsymbol{\theta}}^{k}_{t}$ contributing to the plastic velocity gradient were introduced in (7) and (8), while the *net geometrically necessary* defect density tensors $\boldsymbol{\alpha}$ and $\boldsymbol{\theta}$ (these include both mobile and immobile defects) were formally introduced in (31) and (32). Notice that when $\mathbf{Q} = \mathbf{0}$ (no disclinations) and $\boldsymbol{F}^{\boldsymbol{i}} = \mathbf{1}$, we have $\tilde{\alpha}^{\alpha\beta} \equiv J^{e}F^{e-1\alpha}_{.a}e^{abc}F^{e-1\beta}_{.c,b} = J^{p-1}F^{p\alpha}_{.A}e^{ABC}F^{p\beta}_{.C,B}$, meaning that (45) agrees with constitutive assumptions made in previous gradient-based dislocation theories from the literature (cf. Steinmann, 1996; Regueiro et al., 2002). Since, as mentioned already in Section 2, the tensors $\tilde{\boldsymbol{\alpha}}$ and $\tilde{\boldsymbol{\theta}}$ in (45) do not include a measure of the total length of all dislocation and disclination lines within a given volume element (examples include statistically stored defects consisting of closed loops and tangent lines of opposing signs), the scalar parameters $\tilde{\varepsilon}_{\rho} \equiv b\sqrt{\tilde{\rho}_{S}}$ and $\tilde{\varepsilon}_{\eta} \equiv r\omega\sqrt{\tilde{\eta}_{S}}$ are incorporated to model the net contributions of the elastic self-energy of the statistically stored dislocation density (line length per unit volume in $\tilde{b}$), $\tilde{\rho}_{S}$, and the statistically stored disclination density (also a line length per unit volume in $\tilde{b}$), $\tilde{\eta}_{S}$, to the free energy. We regard $\tilde{\varepsilon}_{\rho}$ and $\tilde{\varepsilon}_{\eta}$ as local residual lattice strain measures associated with these defects (Bammann, 2001). Please notice that heterogeneity of lattice deformation (reflected in (45) by $\mathbf{V}^{\mathbf{i}}$, $\tilde{\boldsymbol{\alpha}}$,

and $\tilde{\boldsymbol{\theta}}$) is not essential to engender substantial energy storage, as $\tilde{\varepsilon}_\rho$ and $\tilde{\varepsilon}_\eta$ account for a large fraction of the observed stored energy of cold working under conditions of homogeneous plastic flow and increase in its magnitude with the accumulation of the average plastic deformation, $\mathbf{F}^{\mathbf{p}}$. Rather, these tensorial variables tend to reflect scale effects, particularly the latter two. Additionally, in an effective sense, $\mathbf{V}^{\mathbf{i}}$ in (45) accounts for higher order moments of distributions of lattice defects within the volume element that lead to internal heterogeneity, such as dislocation pile-ups, for example, that are not accounted for by the first-order averages over the volume element of defect fields $\tilde{\boldsymbol{\alpha}}$, $\tilde{\boldsymbol{\theta}}$, $\tilde{\varepsilon}_\rho$, and $\tilde{\varepsilon}_\eta$. Reasoning for inclusion of metric $\tilde{\mathbf{g}}$ will become clear later. Each variable in (45) is considered invariant with respect to changes in the spatial frame of reference. We choose not to include the rotational part $\mathbf{R}^{\mathbf{i}}$ of $\mathbf{F}^{\mathbf{i}}$ in the free energy function because material rotations of a local volume element in unloaded configuration $\tilde{b}$, while affecting orientations of the lattice directors via (15), do not influence the amount of stored elastic energy contained within that element.

We note that the presence of $\mathbf{V}^{\mathbf{i}}$, $\tilde{\boldsymbol{\alpha}}$, and $\tilde{\boldsymbol{\theta}}$ in the free energy function allows for contribution of surface or interfacial energy of grain boundaries, for example, in manifesting certain length scale (surface area to bulk volume) effects on flow stress, provided the dislocation–disclination content of such boundaries is described. Such effects are dominant for nanocrystalline materials.

The dissipation inequality (44) may be re-written as follows, upon introduction of generalized second-rank thermodynamic forces $\tilde{\boldsymbol{\sigma}}$ and $\tilde{\boldsymbol{\mu}}$:

$$\dot{\tilde{\psi}} \leqslant \tilde{L}^{\alpha}_{.\beta}\tilde{M}^{T\beta}_{.\alpha} - \tilde{\psi}\dot{\tilde{F}}^{\alpha}_{.A}\tilde{F}^{-1A}_{.\alpha} - \frac{1}{T}(\tilde{q}^{\alpha}T_{,\alpha}) - \tilde{N}\dot{T} + \underbrace{\tilde{\sigma}_{\alpha\beta}\dot{\tilde{\alpha}}^{\alpha\beta}_{T}}_{=0} + \underbrace{\tilde{\mu}_{\alpha\beta}\dot{\tilde{\theta}}^{\alpha\beta}_{T}}_{=0}, \tag{46}$$

where the final two terms vanish upon consideration of the material time derivative of Eqs. (38). Substituting (45) into (46) and assuming that (46) must hold as $\tilde{\mathbf{C}}^{\mathbf{e}}$ and T are varied independently of the other constitutive variables (e.g., a reversible thermoelastic process), we arrive at the usual constitutive relations, i.e.,

$$\tilde{S}^{\alpha\beta} \equiv 2\frac{\partial\tilde{\psi}}{\partial\tilde{C}^{e}_{\alpha\beta}} = J^{e}F^{e-1\alpha}_{.a}\Sigma^{ab}F^{e-1\beta}_{.b}, \quad \tilde{N} = -\frac{\partial\tilde{\psi}}{\partial T}, \tag{47}$$

with $\tilde{\mathbf{S}}$ a macroscopic elastic second Piola–Kirchhoff stress, as well as the strong form of the reduced dissipation inequality,

$$\begin{aligned}
&\left\langle \tilde{\mathbf{P}}, \tilde{\mathbf{L}}^{\mathbf{p}} \right\rangle + \left\langle \mathbf{P}\tilde{\mathbf{V}}^{\mathbf{i}-1}, \dot{\mathbf{V}}^{\mathbf{i}} \right\rangle + \left\langle \mathbf{V}^{\mathbf{i}}\mathbf{P}\tilde{\mathbf{V}}^{\mathbf{i}-1}, \tilde{\mathbf{W}}^{\mathbf{i}} \right\rangle + \left\langle \tilde{\boldsymbol{\sigma}}^{\mathrm{T}}, \dot{\tilde{\boldsymbol{\alpha}}}_{\mathbf{p}} \right\rangle + \left\langle \tilde{\boldsymbol{\mu}}^{\mathrm{T}}, \dot{\tilde{\boldsymbol{\theta}}}_{\mathbf{p}} \right\rangle \\
&\quad \geqslant \left\langle \frac{\partial\tilde{\psi}}{\partial\mathbf{V}^{\mathbf{i}}}, \dot{\mathbf{V}}^{\mathbf{i}} \right\rangle + \left\langle \left(\frac{\partial\tilde{\psi}}{\partial\tilde{\boldsymbol{\alpha}}}\right)^{\mathrm{T}} - \tilde{\boldsymbol{\sigma}}^{\mathrm{T}}, \dot{\tilde{\boldsymbol{\alpha}}} \right\rangle + \left\langle \left(\frac{\partial\tilde{\psi}}{\partial\tilde{\boldsymbol{\theta}}}\right)^{\mathrm{T}} - \tilde{\boldsymbol{\mu}}^{\mathrm{T}}, \dot{\tilde{\boldsymbol{\theta}}} \right\rangle \\
&\qquad + \frac{\partial\tilde{\psi}}{\partial\tilde{\varepsilon}_\rho}\dot{\tilde{\varepsilon}}_\rho + \frac{\partial\tilde{\psi}}{\partial\tilde{\varepsilon}_\eta}\dot{\tilde{\varepsilon}}_\eta + \left\langle \frac{\partial\tilde{\psi}}{\partial\tilde{\mathbf{g}}}, \dot{\tilde{\mathbf{g}}} \right\rangle,
\end{aligned} \tag{48}$$

where the spin $\tilde{\mathbf{W}}^{\mathbf{i}}$ and plastic velocity gradient $\tilde{\mathbf{L}}^{\mathbf{p}}$ referred to configuration $\tilde{b}$ are found from

$$\dot{\mathbf{F}}^{\mathbf{i}}\mathbf{F}^{\mathbf{i}-1} = \dot{\mathbf{V}}^{\mathbf{i}}\mathbf{V}^{\mathbf{i}-1} + \mathbf{V}^{\mathbf{i}}\underbrace{\dot{\mathbf{R}}^{\mathbf{i}}\mathbf{R}^{\mathbf{i}T}}_{\tilde{\mathbf{W}}^{\mathbf{i}}}\mathbf{V}^{\mathbf{i}-1}, \quad \tilde{\mathbf{L}}^{\mathbf{p}} = \mathbf{F}^{\mathbf{i}}\dot{\mathbf{F}}^{\mathbf{p}}\mathbf{F}^{\mathbf{p}-1}\mathbf{F}^{\mathbf{i}-1}, \tag{49}$$

and where the Eshelby-type stress (cf. Eshelby, 1951, 1975; Maugin, 1994; Le and Stumpf, 1996c),

$$\tilde{\mathbf{P}} \equiv \tilde{\mathbf{M}}^{\mathrm{T}} - \tilde{\psi}\tilde{\mathbf{1}} = J^{e}\mathbf{F}^{\mathbf{e}-1}\underbrace{(\boldsymbol{\Sigma}\mathbf{g} - \psi\mathbf{1})}_{\mathbf{p}}\mathbf{F}^{\mathbf{e}} = \tilde{J}^{-1}\tilde{\mathbf{F}}\underbrace{\left(\mathbf{F}^{\mathrm{T}}\hat{\mathbf{T}}G - \psi_0\mathbf{1}_0\right)}_{\mathbf{P}}\tilde{\mathbf{F}}^{-1} \tag{50}$$

is defined as the push-forward of the mixed-variant reference configuration energy-momentum tensor $\mathbf{P}$, or equivalently as the pull-back of the current configuration Eshelby stress tensor $\mathbf{p}$. In Eq. (50), $\mathbf{1}_0$, $\tilde{\mathbf{1}}$, and $\mathbf{1}$ denote mixed-variant identity maps on configurations $b_0, \tilde{b}$, and b, respectively, $\hat{T} = S^{\mathrm{T}}$ is the usual first Piola–Kirchhoff stress, $\tilde{\mathbf{M}}^{\mathrm{T}}$ is the transposed Mandel stress, $\mathbf{g}$ is the current configuration metric tensor, $\mathbf{G}$ is the reference configuration metric tensor, and ψ is the free energy measured per unit current volume. We enforce the notion that the geometrically necessary defect density tensors $\tilde{\boldsymbol{\alpha}}$ and $\tilde{\boldsymbol{\theta}}$ contribute neither storage or dissipation on the right side of (48), resulting in

$$\tilde{\boldsymbol{\sigma}} = \frac{\partial\tilde{\psi}}{\partial\tilde{\boldsymbol{\alpha}}}, \quad \tilde{\boldsymbol{\mu}} = \frac{\partial\tilde{\psi}}{\partial\tilde{\boldsymbol{\theta}}}, \tag{51}$$

and leading to

$$\underbrace{\left\langle \tilde{\mathbf{P}}, \tilde{\mathbf{L}}^{\mathbf{p}} \right\rangle}_{\substack{\text{Dissipation from}\\ \text{plastic defect fluxes}\\ \text{(e.g. dislocation glide)}}} + \underbrace{\left\langle \tilde{\mathbf{P}}\mathbf{V}^{\mathbf{i}-1}, \dot{\mathbf{V}}^{\mathbf{i}} \right\rangle}_{\substack{\text{Dissipation from}\\ \text{microscopic heterogeneity}\\ \text{(e.g. dislocation clustering)}}} + \underbrace{\left\langle \mathbf{V}^{\mathbf{i}}\tilde{\mathbf{P}}\mathbf{V}^{\mathbf{i}-1}, \tilde{\mathbf{W}}^{\mathbf{i}} \right\rangle}_{\substack{\text{Dissipation from}\\ \text{microscopic heterogeneity}\\ \text{(e.g. disclination spin)}}} + \underbrace{\left\langle \tilde{\boldsymbol{\sigma}}^{\mathrm{T}}, \dot{\tilde{\boldsymbol{\alpha}}}_{\mathbf{p}} \right\rangle + \left\langle \tilde{\boldsymbol{\mu}}^{\mathrm{T}}, \dot{\tilde{\boldsymbol{\theta}}}_{\mathbf{p}} \right\rangle}_{\substack{\text{Dissipation from}\\ \text{geometrically necessary defect densities}}}$$

$$\geqslant \underbrace{\left\langle \frac{\partial\tilde{\psi}}{\partial\mathbf{V}^{\mathbf{i}}}, \dot{\mathbf{V}}^{\mathbf{i}} \right\rangle}_{\substack{\text{Energy storage from}\\ \text{microscopic heterogeneity}}} + \underbrace{\frac{\partial\tilde{\psi}}{\partial\tilde{\varepsilon}_{\rho}}\dot{\tilde{\varepsilon}}_{\rho} + \frac{\partial\tilde{\psi}}{\partial\tilde{\varepsilon}_{\eta}}\dot{\tilde{\varepsilon}}_{\eta}}_{\substack{\text{Energy storage from}\\ \text{statistically stored defect densities}}} + \underbrace{\left\langle \frac{\partial\tilde{\psi}}{\partial\tilde{\mathbf{g}}}, \dot{\tilde{\mathbf{g}}} \right\rangle}_{\substack{\text{Choice of}\\ \text{intermediate metric tensor}}}. \tag{52}$$

We have described the physics behind each term in (52) apart from the final term related to $\tilde{\mathbf{g}}$. If we make the (usual) constitutive assumption $\tilde{g}_{\alpha\beta} = \delta_{\alpha\beta}$, where $\delta_{\alpha\beta}$ is the covariant identity map, this term vanishes. As discussed by Clayton et al. (2004b), other choices for $\tilde{g}_{\alpha\beta}$ may be advantageous for describing situations in which internal stresses associated with defect arrangements (e.g., at flexing subgrain walls) may arise from or be amplified by applied loads (Gibeling and Nix, 1980; Argon and Takeuchi, 1981; Kassner et al., 2002). Additionally, note that from (38) we have $\langle \tilde{\boldsymbol{\sigma}}^{\mathrm{T}}, \dot{\tilde{\boldsymbol{\alpha}}}_{\mathbf{p}} \rangle = -\langle \tilde{\boldsymbol{\sigma}}^{\mathrm{T}}, \dot{\tilde{\boldsymbol{\alpha}}} \rangle$ and $\langle \tilde{\boldsymbol{\mu}}^{\mathrm{T}}, \dot{\tilde{\boldsymbol{\theta}}}_{\mathbf{p}} \rangle = -\langle \tilde{\boldsymbol{\mu}}^{\mathrm{T}}, \dot{\tilde{\boldsymbol{\theta}}} \rangle$, meaning that the final two terms on the left-hand side of inequality (52) may be replaced by terms denoting energy storage associated with geometrically necessary defects (see later Eq. (90)), as a matter of preference in addressing the issue of energy storage versus dissipation as a function of scale (cf. Wei and Hutchinson, 1999).

The general philosophy adopted here is prescription of balance laws for the energetic forces $\boldsymbol{\Sigma}$ (macroscopic Cauchy stress), $\tilde{\boldsymbol{\sigma}}$ (microscopic force conjugate to

geometrically necessary dislocations within the volume element), and $\tilde{\boldsymbol{\mu}}$ (microscopic force conjugate to geometrically necessary disclinations within the volume element) as well as the temperature T. Additional evolution equations are then required to specify the time history of dissipative kinematic variables $\mathbf{F}^{\mathbf{i}}$ and $\mathbf{F}^{\mathbf{p}}$ and scalar internal variables $\tilde{\varepsilon}_\rho$ and $\tilde{\varepsilon}_\eta$. Force conjugates $\frac{\partial\tilde{\psi}}{\partial\mathbf{V}^{\mathbf{i}}}$, $\frac{\partial\tilde{\psi}}{\partial\tilde{\varepsilon}_\rho}$, and $\frac{\partial\tilde{\psi}}{\partial\tilde{\varepsilon}_\eta}$ associated in (52) with energy storage (i.e., residual energy from cold working) are not required to satisfy any additional balance laws.

From (39) to (41), the macroscopic Cauchy stress $\boldsymbol{\Sigma}$ is supposed to obey the standard linear and angular momentum balances and reflects the average traction carried by a local crystalline volume element in the current configuration. The microforces $\tilde{\boldsymbol{\sigma}}$ and $\tilde{\boldsymbol{\mu}}$ reflect higher order moments of the microscopic traction distribution supported by the volume element (see e.g., Kröner, 1963) and do not explicitly enter the macroscopic momentum (41) or energy (42) balances in our theory. Instead, contravariant mixed-configurational versions of these forces,

$$\sigma^{\bar{\alpha}b} \equiv J^{e-1}F^{i-1\bar{\alpha}}_{\ \ .\alpha}\tilde{g}^{\alpha\chi}\tilde{\sigma}_{\chi\delta}\tilde{g}^{\beta\delta}F^{eb}_{\ \ .\beta}, \quad \mu^{\bar{\alpha}b} \equiv J^{e-1}F^{i-1\bar{\alpha}}_{\ \ .\alpha}\tilde{g}^{\alpha\chi}\tilde{\mu}_{\chi\delta}\tilde{g}^{\beta\delta}F^{eb}_{\ \ .\beta}, \tag{53}$$

satisfy coupled microscopic momentum balances independent from (40). The higher order microscopic balance relations are intended to apply to subvolumes within the considered macroelement pertinent to the macroscopic momentum balance relations in (41). At these finer scales, heterogeneous features such as grains, second phases, subgrains, or other dislocation substructures are expected to engender gradients of $\tilde{\boldsymbol{\alpha}}$ and $\tilde{\boldsymbol{\theta}}$. This clarification of macro- and micro-effectively parallels the kinematical argument of Section 2 in that $\mathbf{F}^{\mathbf{i}}$ reflects heterogeneity at subscales within the considered volume element subjected to the multiplicative deformation gradient decomposition $\mathbf{F} = \mathbf{F}^{\mathbf{e}}\mathbf{F}^{\mathbf{i}}\mathbf{F}^{\mathbf{p}} = \mathbf{F}^{\mathscr{L}}\mathbf{F}^{\mathbf{p}}$.

Please note that $\boldsymbol{\sigma}$ is a first-order moment stress (i.e., couple stress) with units of *Force*/*Length*, whereas $\boldsymbol{\mu}$ is a second-order moment stress (i.e., hyperstress) with units of *Force*. Extending standard stress tetrahedron arguments for micropolar media with higher-order stresses (cf. Malvern, 1969), we postulate the following global angular momentum balances, restricted here to the microscopically quasi-static case (i.e., no micro-inertia) and in the absence of microscopic body forces:

$$\int_a \bar{\mathbf{t}}_{\boldsymbol{\sigma}}\,\mathrm{d}a = \mathbf{0}, \quad \int_a \left(\bar{\boldsymbol{\varepsilon}} : (\bar{\mathbf{x}} \otimes \bar{\mathbf{t}}_{\boldsymbol{\sigma}}) + \bar{\mathbf{t}}_{\mu}\right)\mathrm{d}a = \mathbf{0}, \tag{54}$$

where $\bar{\mathbf{t}}_{\boldsymbol{\sigma}} = \langle\boldsymbol{\sigma}, \mathbf{n}\rangle$ and $\bar{\mathbf{t}}_{\boldsymbol{\mu}} = \langle\boldsymbol{\mu}, \mathbf{n}\rangle$ are, respectively, first- and second-order couple traction vectors with components referred to $\bar{b}$ and acting on spatial surface a with outward normal $\mathbf{n}$, and $\bar{\mathbf{x}} \equiv \mathbf{F}^{\mathscr{L}-1}\mathbf{x}$ are spatial coordinates pulled back to $\bar{b}$ under the Cauchy–Born approximation. Localized forms of (54) then follow naturally from application of the divergence theorem in the current configuration:

$$\sigma^{\bar{\alpha}b}_{\ \ |b} = 0, \quad \bar{\varepsilon}_{\bar{\alpha}\bar{\beta}\bar{\chi}}F^{\mathscr{L}-1\bar{\beta}}_{\ \ .b}\sigma^{\bar{\chi}b} + \mu^{b}_{\bar{\alpha}|b} = 0, \tag{55}$$

where $\mu^{a}_{\bar{\alpha}} = \bar{g}_{\bar{\alpha}\bar{\beta}}\mu^{\bar{\beta}a}$ and vertical bars denote covariant differentiation with respect to spatial coordinates $\mathbf{x}$. Relations (55) are analogous to the micropolar elastic balance laws used in the finite strain theory of Minagawa (1979) and the linearized theory of Eringen and Claus (1970). We note that if $\tilde{\psi}$ is quadratic in each of $\tilde{\boldsymbol{\alpha}}$ and $\tilde{\boldsymbol{\theta}}$, then $\boldsymbol{\sigma}$

and $\boldsymbol{\mu}$ in (55) are, respectively, linear in configurational mappings of $\tilde{\boldsymbol{\alpha}}$ and $\tilde{\boldsymbol{\theta}}$, and the so-called "microforce balances" in (55) are then interpreted in terms of covariant spatial gradients of geometrically necessary dislocations $(55)_1$, pertaining to pile-ups and dipole structures, and disclinations $(55)_2$, contributing to nonsymmetric moment stress $\tilde{\boldsymbol{\sigma}}$.

The usual heat equation is suggested for the temperature field:

$$q^A = -kT_{|B}G^{BA}, \tag{56}$$

where we have assumed isotropic conduction (a typical assumption easily extended to the anisotropic case), with thermal conductivity k, posed above in the reference coordinate frame.

The time rate of $\mathbf{F^p}$ is described by Eq. (9), i.e., $\dot{\mathbf{F}}^{\mathbf{p}} = \bar{\mathbf{L}}^{\mathbf{p}}\mathbf{F}^{\mathbf{p}}$, which in turn requires constitutive equations for slip rates $\dot{\gamma}^i$ of (10). In rate dependent crystals, slip is typically dictated by a viscoplastic flow rule, in our case of the following form in configuration $\bar{b}$:

$$\dot{\gamma}^i = \dot{\gamma}^i\left(\bar{p}^j, \bar{\rho}_S^j, \bar{\eta}_S^j, \bar{\boldsymbol{\alpha}}, \bar{\boldsymbol{\theta}}, \mathbf{U}^{\mathbf{i}}, T\right), \tag{57}$$

where the driving force for slip, $\bar{p}^i \equiv \bar{m}^i_{\bar{\alpha}} F^{i-1\bar{\alpha}}_{\quad .\alpha} \tilde{P}^{\alpha}_{\quad .\beta} F^{i\beta}_{\quad .\bar{\beta}} \bar{s}^{i\bar{\beta}}$, is a resolved scalar Eshelby stress on system i such that

$$\left\langle \tilde{\mathbf{P}}, \mathbf{F}^{\mathbf{i}} \left(\sum_i \dot{\gamma}^i \bar{\mathbf{s}}^i \otimes \bar{\mathbf{m}}^i \right) \mathbf{F}^{\mathbf{i}-1} \right\rangle = \sum_i \bar{p}^i \dot{\gamma}^i \tag{58}$$

is the contribution of the plastic shearing rates to the dissipation inequality (52). The variables $\bar{\rho}_S^i$ and $\bar{\eta}_S^i$ are statistically stored defect densities assigned to the i^{th} slip system, i.e., line lengths per unit volume in configuration $\bar{b}$, such that

$$J^i \tilde{\rho}_S \equiv \bar{\rho}_S = \sum_i \bar{\rho}_S^i, \quad J^i \tilde{\eta}_S \equiv \bar{\eta}_S = \sum_i \bar{\eta}_S^i, \tag{59}$$

with J^i the Jacobian determinant of $\mathbf{F}^{\mathbf{i}}$. In (57), statistically stored defects generally contribute to self-hardening ($i = j$) and latent-hardening ($i \neq j$). Geometrically necessary defect densities also contribute to hardening on each system, and as a result, their counterparts in configuration $\bar{b}$, defined as

$$\bar{\alpha}^{\bar{\alpha}\bar{\beta}} \equiv J^i F^{i-1\bar{\alpha}}_{\quad .\alpha} \tilde{\alpha}^{\alpha\beta} F^{i-1\bar{\beta}}_{\quad .\beta}, \quad \bar{\theta}^{\bar{\alpha}\bar{\beta}} \equiv J^i F^{i-1\bar{\alpha}}_{\quad .\alpha} \tilde{\theta}^{\alpha\beta} F^{i-1\bar{\beta}}_{\quad .\beta}, \tag{60}$$

are included in the flow rule (57). Please note that the *net* defect density tensors in (60) are not to be confused with the *total* defect density tensors $\bar{\boldsymbol{\alpha}}_t^j$ and $\bar{\boldsymbol{\theta}}_t^k$ introduced in Eq. (8). It is also noted that within our framework, the plastic velocity gradient may alternatively be described by evolution laws for defect fluxes and generation rates of Eqs. (7) or (10) (cf. Acharya (2001, 2003)) rather than evolution equations for slip rates as in (57). The former approach appears more conducive to correlation with numerical experiments based on discrete dislocation dynamics (cf. Zbib and De La Rubia, 2002) or atomic-scale interactions (cf. Nazarov et al., 2000), while the latter approach appears more conducive to correlation with macroscopic experiments.

Specific guidelines describing how dislocation densities may participate in the flow rule (i.e., strain hardening) can be found in previous works by the co-authors (Bammann, 2001; Regueiro et al., 2002; Clayton et al., 2004a). Disclination densities (specifically, partial disclination dipoles) may contribute to hardening and/or geometrical softening depending upon the particular material under consideration and its deformation history, as discussed by Pęcherski (1983, 1985) and Seefeldt and co-workers (Seefeldt and Klimanek, 1997, 1998; Seefeldt, 2001). The right stretch tensor $\mathbf{U}^{\mathbf{i}}$ of $\mathbf{F}^{\mathbf{i}}$ (i.e., the counterpart of left stretch $\mathbf{V}^{\mathbf{i}}$ in configuration $\bar{b}$) is included in (57) to account for contributions of heterogeneity of inelastic deformation within the local volume not engendered by that volume's (average) statistically stored and geometrically necessary defect densities, such as higher order moments of dislocation densities (Kröner, 1973; Hartley, 1975) contained within the element. For example, a backstress may arise in conjunction with piled-up dislocations at a misoriented subgrain boundary. The corresponding inhibiting effect on plastic flow would then manifest in (57) through the inclusion of $\bar{\boldsymbol{\theta}}$ and $\mathbf{U}^{\mathbf{i}}$, the former reflecting the misorientation boundary itself and the latter accounting for a spatial gradient of dislocation density in the pile-up direction. Our treatment could be further extended to explicitly include higher order gradients or moments of defect densities in the flow rule or yield conditions, albeit at the expense of increased model complexity. Also, when inelastic volume changes are of interest (e.g., high temperature creep conditions characterized by vacancy migration), a nonvanishing non-slip term $\bar{\mathbf{L}}_{\mathbf{v}}^{\mathbf{p}}$ should be included in kinematic relation (9), with its evolution exhibiting the same general constitutive dependency as $\dot{\gamma}^i$ in (57).

Since statistically stored defects accumulate in response to the motion of defects and their interactions, their evolution equations are assigned the same general constitutive dependencies as the shearing rates, i.e.,

$$\dot{\bar{\rho}}_S^i = \dot{\bar{\rho}}_S^i\left(\bar{p}^j, \bar{\rho}_S^j, \bar{\eta}_S^j, \bar{\boldsymbol{\alpha}}, \bar{\boldsymbol{\theta}}, \mathbf{U}^{\mathbf{i}}, T\right), \quad \dot{\bar{\eta}}_S^i = \dot{\bar{\eta}}_S^i\left(\bar{p}^j, \bar{\rho}_S^j, \bar{\eta}_S^j, \bar{\boldsymbol{\alpha}}, \bar{\boldsymbol{\theta}}, \mathbf{U}^{\mathbf{i}}, T\right). \tag{61}$$

Kinetic relations such as (61) are strongly material dependent. More specific equations dealing with coupled evolution of dislocation and disclination densities – which may be considered as particular implementations of the general relations (61) – may be found in the cited references (Pęcherski, 1983, 1985; Seefeldt and Klimanek, 1997, 1998; Seefeldt, 2001). An analogous general prescription is given for the time rate of $\mathbf{F}^{\mathbf{i}}$, referred to configuration $\bar{b}$:

$$\mathbf{F}^{\mathbf{i}-\mathbf{1}}\dot{\mathbf{F}}^{\mathbf{i}} \equiv \bar{\mathbf{L}}^{\mathbf{i}} = \bar{\mathbf{L}}^{\mathbf{i}}\left(\bar{\mathbf{P}}, \bar{\rho}_S^i, \bar{\eta}_S^i, \bar{\boldsymbol{\alpha}}, \bar{\boldsymbol{\theta}}, \mathbf{U}^{\mathbf{i}}, T\right), \tag{62}$$

where $\bar{P}^{\bar{\alpha}}_{\ .\bar{\beta}} \equiv F^{i-1\bar{\alpha}}_{\ \ .\alpha}\tilde{P}^{\alpha}_{\ .\beta}F^{i\beta}_{\ \ .\bar{\beta}}$ is the Eshelby stress tensor on $\bar{b}$. As introduced in Eq. (12), $\mathbf{F}^{\mathbf{i}}$ accounts for lattice heterogeneity within the crystalline volume element and also dictates the rate of rotation of the slip planes and directions arising from the generation and flux of mobile disclinations traversing the element, and as a result, will account for the diffusion of crystallographic texture observed as subgrain cells – delineated in our present framework by walls of partial disclination dipoles – emerge and then rotate relative to one another (see e.g., Butler and McDowell, 1998; Peeters et al., 2001; Hughes et al., 2003). From Fig. 4 and the definition $\mathbf{F}^{\mathscr{L}} \equiv \mathbf{F}^{\mathbf{e}}\mathbf{F}^{\mathbf{i}}$, the rotational part $\mathbf{R}^{\mathbf{e}}$ of $\mathbf{F}^{\mathbf{e}}$ depicts the average rotation undergone by the lattice between unloaded state $\tilde{b}$

and the current configuration b, while the rotational part $\mathbf{R}^{\mathbf{i}}$ of $\mathbf{F}^{\mathbf{i}}$ accounts for additional rotation of the lattice due to defect fields embedded within the material in relaxed configuration $\tilde{b}$. Notice also that $\mathbf{F}^{\mathbf{i}}$ affects the slip system orientations through its inclusion in the total lattice deformation $\mathbf{F}^{\mathscr{L}}$, since the slip directions $\mathbf{s}^i$ and slip plane normals $\mathbf{m}^i$ are pushed forward to current configuration b from intermediate configuration $\bar{b}$ as

$$\mathbf{s}^i = \mathbf{F}^{\mathscr{L}}\bar{\mathbf{s}}^i, \quad \mathbf{m}^i = \bar{\mathbf{m}}^i\mathbf{F}^{\mathscr{L}-1}. \tag{63}$$

The specific form of the constitutive equation for $\bar{\mathbf{L}}^{\mathbf{i}}$ for a given material and scale of resolution (e.g., ℓ_{ref} in (1)) depends upon the particular arrangement of defects within the crystal and how their local lattice strain fields interact and contribute to the motion of the element's external boundary. Discrete dislocation simulations or atomistic studies conducted in a manner analogous to the continuum simulations described in Clayton and McDowell (2003) are expected to provide more insight into developing Eq. (62) for particular materials.

The micropolar kinematic variable $\mathbf{Q}$ describes spatial gradients of lattice rotation within the crystalline volume element arising from distributed disclinations. Consider parallel transport of the lattice director $\mathbf{d}_a$, over the small distance $d\mathbf{x}$ to a new orientation $\mathbf{d}'_a$, conducted with respect to the covariant derivative (19). To isolate the effects of $\mathbf{Q}$, we restrict attention now to the case when $\mathbf{F}^{\mathscr{L}} \approx \mathbf{1}$ and spatial gradients of the lattice deformation $\mathbf{F}^{\mathscr{L}}$ are small. Applying the summation convention over covariant Cartesian coordinates, we then may write

$$\mathbf{d}'_a = \mathbf{d}_a + \mathbf{d}_{a,b}dx_b = \mathbf{d}_a + Q_{bac}dx_b\mathbf{d}_c = \left(\delta_{ac} + Q_{b[ac]}dx_b\right)\mathbf{d}_c = \Phi_{ac}\mathbf{d}_c, \tag{64}$$

where $Q_{bac} = Q_{b[ac]}$ from Eq. (21), and the rotation matrix Φ_{ac} satisfies $\mathbf{\Phi}^{\mathrm{T}} \approx \mathbf{\Phi}^{-1}$ and $\det(\mathbf{\Phi}) \approx 1$ for small magnitudes of $Q_{bac}dx_b$, i.e., small relative lattice rotations such as those occurring across low-angle grain boundaries. We see from (64) that Q_{bac} acts as an effective "gradient" of rotation in the spatial direction x_b. However, $\mathbf{Q}$ is not a *true* spatial gradient since $Q_{b[ac],d} - Q_{d[ac],b} \neq 0 \rightarrow Q_{b[ac]} \neq \vartheta_{[ac],b}$, where $\vartheta_{[ac]}$ is a skew matrix that can exist only when the compatibility conditions $Q_{b[ac],d} = Q_{d[ac],b}$ are met. From Eq. (26) and the second of (29), enforcement of such conditions would in fact yield a null disclination density $\boldsymbol{\theta}$ in the context of linear approximation (64). Note that the nine independent degrees-of-freedom of $\mathbf{Q}$ could be determined, in principle, from knowledge of incremental changes in lattice rotation due to disclinations, based upon measured gradients of intragranular misorientation, sometimes referred to as "disorientation" (Barton and Dawson, 2001; Bergugnat, 2002; Kassner et al., 2002).

Our framework is complete upon introduction of explicit relationships between the macroscopic rotation attributed to defects, $\mathbf{R}^{\mathbf{i}}$, and the microscopic defect density measures, e.g.,

$$\mathbf{R}^{\mathbf{i}} = \mathbf{R}^{\mathbf{i}}\left(\tilde{\boldsymbol{\alpha}}, \tilde{\boldsymbol{\theta}}, \tilde{\varepsilon}_\rho, \tilde{\varepsilon}_\eta\right). \tag{65}$$

Please notice that (65) is introduced independently of kinetic relation (62), the latter implicitly containing an evolution equation for the spin due to the time rate of $\mathbf{R}^{\mathbf{i}}$,

i.e., $\tilde{\mathbf{W}}^{\mathbf{i}}$ of (49), which in turn contributes to the dissipation rate in (52) but not to energy storage in $\tilde{\psi}$ of (45). Also note that no corresponding kinematic equation analogous to (65) is given for the stretch $\mathbf{V}^{\mathbf{i}}$, which is included explicitly in the free energy function of (45) to account for higher order moments of distirubutions of lattice defects that lead to internal heterogeneity of lattice deformation within the local volume element, such as dislocation pile-ups, for example, that are not accounted for by variables $\tilde{\boldsymbol{\alpha}}$, $\tilde{\boldsymbol{\theta}}$, $\tilde{\varepsilon}_{\rho}$, and $\tilde{\varepsilon}_{\eta}$. A variant of (65) follows from Lardner (1973, 1974), if we assume that $\mathbf{R}^{\mathbf{i}}$ is determined by the change in orientation of a lattice director vector upon parallel transport around a closed circuit encircling area a:

$$R^{i\alpha}_{\cdot\bar{\beta}} \equiv \delta^{\alpha}_{a}\left(\delta^{a}_{b} + \int_{a} \frac{1}{2} R^{a}_{bcd}\varepsilon^{cde} n_e \,\mathrm{d}a\right)\delta^{b}_{\beta} = \delta^{\alpha}_{\beta} + \delta^{\alpha}_{a}\delta^{e}_{\beta}\int_{a} C^{\mathscr{L}-1ab}\varepsilon_{beg}\theta^{gh}n_h \,\mathrm{d}a$$
$$\approx \delta^{\alpha}_{\beta} + \delta^{\alpha}_{a}\delta^{e}_{\beta}C^{\mathscr{L}-1ab}\varepsilon_{beg}\Omega^{g} \tag{66}$$

where δ^{α}_{a} and δ^{b}_{β} are shifters between coincident Cartesian spatial and intermediate frames, and where in the final equality of (66), we have assumed a constant lattice stretch over a, such that the net Frank vector $\Omega^{g} = \int_{a}\theta^{gh}n_h \,\mathrm{d}a$ plays the role of the axial vector corresponding to the rotation tensor $\mathbf{R}^{\mathbf{i}}$ in (66), rigorously orthogonal only in the limit of small rotations. Notice that definition (66) is non-unique in the sense that $\mathbf{R}^{\mathbf{i}}$ depends upon the choice of oriented area element $\mathbf{n}\mathrm{d}a$. In our crystal plasticity framework, it is natural to generalize the second of (66) to a discrete average taken over potentially active slip planes, as $\mathbf{R}^{\mathbf{i}}$ contributes to the average rotation of the lattice directors and the slip planes (e.g., Eqs. (15) and (63)). Such an approach gives

$$R^{i\alpha}_{\cdot\bar{\beta}} = \delta^{\alpha}_{\beta} + \delta^{\alpha}_{a}\delta^{e}_{\beta}C^{\mathscr{L}-1ab}\varepsilon_{beg}\left(\frac{\ell^{2}_{\mathrm{ref}}}{k}\sum_{i=1}^{k}\theta^{gh}(m^{i})_{h}\right), \tag{67}$$

where k is the number of slip systems and the factor ℓ^{2}_{ref} corresponds to the effective area over which the disclinations act. In the limit that our local crystal volume element shrinks to infinitesimal size, $\ell_{\mathrm{ref}} \to 0$, and effects of disclinations can no longer be resolved by the deformation gradient field. Particular Eq. (67) is deemed an appropriate approximation of (65) under the following conditions: (i) the elastic lattice stretch and net Frank vector are small, (ii) disclinations dominate the net residual lattice rotation relative to geometrically necessary dislocations, and (iii) the net influences on lattice rotation from statistically stored defects contained within the volume element cancel out. Furthermore, when the residual lattice stretch associated with microstructural heterogeneity ($\mathbf{V}^{\mathbf{i}}$) is negligible, (12) reduces to the kinematic description of Lardner (1973, 1974) and Pęcherski (1983, 1985), i.e., $\mathbf{F} = \mathbf{F}^{\mathbf{e}}\mathbf{R}^{\mathbf{i}}\mathbf{F}^{\mathbf{p}}$. On the other hand, in the most general case, the multiplicative decomposition (12) may be extended to $\mathbf{F} = (\mathbf{F}^{\mathbf{e}})(\mathbf{F}^{\mathbf{i}}_{(1)}\mathbf{F}^{\mathbf{i}}_{(2)}\ldots\mathbf{F}^{\mathbf{i}}_{(k)})(\mathbf{F}^{\mathbf{p}}_{(1)}\mathbf{F}^{\mathbf{p}}_{(2)}\ldots\mathbf{F}^{\mathbf{p}}_{(k)})$ where the residual lattice deformation $\mathbf{F}^{\mathbf{i}}$ and lattice-preserving plastic deformation $\mathbf{F}^{\mathbf{p}}$ are each resolved into components associated with k distinct classes of defects (e.g., statistically stored dislocations, geometrically necessary dislocations, disclinations, etc.). Then from (45) and (52), each $\mathbf{F}^{\mathbf{i}}_{(k)}$ would contribute to free energy storage (through a conjugate

thermodynamic force) and dissipation (through the macroscopic stress power), while each $\mathbf{F}^{\mathbf{p}}_{(k)}$ would only contribute to dissipation.

4. Model summary and elements of implementation

Summarized below are the primary relationships comprising the theory, assuming for simplicity isochoric plastic deformation $\bar{\mathbf{L}}^{\mathbf{p}}$ characterized by slip-type kinematics and disclination-dominated residual lattice rotation, $\mathbf{R}^{\mathbf{i}}$:

Macroscopic kinematics

$$\text{(deformation gradient)} \qquad \mathbf{F} = \mathbf{F}^{\mathbf{e}}\mathbf{F}^{\mathbf{i}}\mathbf{F}^{\mathbf{p}} = \mathbf{F}^{\mathscr{L}}\mathbf{F}^{\mathbf{p}}, \tag{68}$$

$$\text{(plastic velocity gradient)} \qquad \bar{\mathbf{L}}^{\mathbf{p}} \equiv \dot{\mathbf{F}}^{\mathbf{p}}\mathbf{F}^{\mathbf{p}-1} = \sum_i \dot{\gamma}^i \bar{\mathbf{s}}^i \otimes \bar{\mathbf{m}}^i, \tag{69}$$

$$\text{(slip system directors)} \qquad \mathbf{s}^i = \mathbf{F}^{\mathscr{L}}\bar{\mathbf{s}}^i, \quad \mathbf{m}^i = \bar{\mathbf{m}}^i\mathbf{F}^{\mathscr{L}-1}, \tag{70}$$

$$\text{(total lattice strain)} \qquad C^{\mathscr{L}}_{ab} = F^{\mathscr{L}-1\bar{\alpha}}_{\ .a}\delta_{\bar{\alpha}\bar{\beta}}F^{\mathscr{L}-1\bar{\beta}}_{\ .b}. \tag{71}$$

Microscopic kinematics

$$\text{(linear connection)} \qquad \Gamma^{..a}_{cb} = F^{\mathscr{L}a}_{\ .\bar{\alpha}}F^{\mathscr{L}-1\bar{\alpha}}_{\ .b,c} + Q^{..a}_{cb}, \tag{72}$$

$$\text{(micro}-\text{rotation)} \qquad Q_{cba} = Q_{c[ba]} = Q^{..d}_{cb}C^{\mathscr{L}}_{da}, \tag{73}$$

$$\text{(torsion/dislocations)} \qquad T^{..a}_{cb} = T^{..a}_{[cb]} = \Gamma^{..a}_{cb} - \Gamma^{..a}_{bc} = \varepsilon_{cbd}\alpha^{ad}, \tag{74}$$

$$\text{(curvature/disclinations)} \qquad \begin{aligned} R_{abcd} = R_{[ab][cd]} &= 2\nabla_{[c}Q_{d][ba]} + T^{..e}_{cd}Q_{e[ba]} \\ &= \varepsilon_{bae}\varepsilon_{cdf}\theta^{ef}. \end{aligned} \tag{75}$$

Micro-macroscopic kinematics

$$\text{(disclination lattice rotation)} \qquad R^{i\alpha}_{\ .\beta} = \delta^{\alpha}_{\beta} + \delta^{\alpha}_{a}\delta^{e}_{\beta}C^{\mathscr{L}-1ab}\varepsilon_{beg}\left(\frac{\ell^2_{\text{ref}}}{k}\sum\nolimits_{i=1}^{k}\theta^{gh}(m^i)_h\right). \tag{76}$$

Macroscopic balance laws

$$\text{(mass)} \qquad \rho_0 = \rho J, \tag{77}$$

$$\text{(linear momentum)} \qquad \boldsymbol{\Sigma}^{ab}{}_{|b} + \rho\hat{f}^{a} = \rho\ddot{x}^a, \tag{78}$$

$$\text{(angular momentum)} \qquad \varepsilon_{abc}\boldsymbol{\Sigma}^{bc} = 0, \tag{79}$$

$$\text{(traction boundary conditions)} \qquad t^a = \boldsymbol{\Sigma}^{ab}n_b. \tag{80}$$

Microscopic balance laws

$$\text{(first order micro} - \text{momentum)} \qquad \sigma^{\bar{\alpha}b}{}_{|b} = 0, \tag{81}$$

$$\text{(second order micro} - \text{momentum)} \qquad \bar{\varepsilon}_{\bar{\alpha}\bar{\beta}\bar{\chi}} F^{\mathscr{P}-1\bar{\beta}}_{.b} \sigma^{\bar{\chi}b} + \mu^{b}_{\bar{\alpha}|b} = 0, \tag{82}$$

$$\text{(traction boundary conditions)} \qquad (\bar{t}_{\sigma})^{\bar{\alpha}} = \sigma^{\bar{\alpha}b} n_b, \qquad (\bar{t}_{\mu})^{\bar{\alpha}} = \mu^{\bar{\alpha}b} n_b. \tag{83}$$

Thermodynamics

$$\text{(free energy)} \qquad \tilde{\psi} = \tilde{\psi}\left(\tilde{\mathbf{C}}^{\mathbf{e}}, \mathbf{V}^{\mathbf{i}}, \tilde{\boldsymbol{\alpha}}, \tilde{\boldsymbol{\theta}}, \tilde{\varepsilon}_{\rho}, \tilde{\varepsilon}_{\eta}, T, \tilde{\mathbf{g}}\right), \tag{84}$$

$$\text{(internal energy rate)} \qquad \dot{U}_0 = S^{Aa} g_{ab} \dot{F}^{b}_{.A} - q^{A}_{|A} + H_0, \tag{85}$$

$$\text{(heat flux)} \qquad q^{A} = -kT_{|B} G^{BA}, \tag{86}$$

$$\text{(macrostress)} \qquad \tilde{S}^{\alpha\beta} \equiv 2\frac{\partial \tilde{\psi}}{\partial \tilde{C}^{e}_{\alpha\beta}} = J^{e} F^{e-1\alpha}_{.a} \boldsymbol{\Sigma}^{ab} F^{e-1\beta}_{.b}, \tag{87}$$

$$\text{(entropy)} \qquad \tilde{N} = -\frac{\partial \tilde{\psi}}{\partial T}, \tag{88}$$

$$\text{(microstresses)} \qquad \tilde{\boldsymbol{\sigma}} = \frac{\partial \tilde{\psi}}{\partial \tilde{\boldsymbol{\alpha}}}, \qquad \tilde{\boldsymbol{\mu}} = \frac{\partial \tilde{\psi}}{\partial \tilde{\boldsymbol{\theta}}}, \tag{89}$$

$$\begin{aligned} &\text{(dissipation inequality)} \qquad \left\langle \tilde{\mathbf{P}}, \tilde{\mathbf{L}}^{\mathbf{p}} \right\rangle + \left\langle \mathbf{P}\tilde{\mathbf{V}}^{\mathbf{i}-1}, \dot{\mathbf{V}}^{\mathbf{i}} \right\rangle + \left\langle \mathbf{V}^{\mathbf{i}}\mathbf{P}\tilde{\mathbf{V}}^{\mathbf{i}-1}, \tilde{\mathbf{W}}^{\mathbf{i}} \right\rangle \\ &\geqslant \left\langle \frac{\partial \tilde{\psi}}{\partial \mathbf{V}^{\mathbf{i}}}, \dot{\mathbf{V}}^{\mathbf{i}} \right\rangle + \left\langle \tilde{\boldsymbol{\sigma}}^{\mathrm{T}}, \dot{\tilde{\alpha}} \right\rangle + \left\langle \tilde{\boldsymbol{\mu}}^{\mathrm{T}}, \dot{\tilde{\boldsymbol{\theta}}} \right\rangle + \frac{\partial \tilde{\psi}}{\partial \tilde{\varepsilon}_{\rho}} \dot{\tilde{\varepsilon}}_{\rho} + \frac{\partial \tilde{\psi}}{\partial \tilde{\varepsilon}_{\eta}} \dot{\tilde{\varepsilon}}_{\eta} + \left\langle \frac{\partial \tilde{\psi}}{\partial \tilde{\mathbf{g}}}, \dot{\tilde{\mathbf{g}}} \right\rangle. \end{aligned} \tag{90}$$

Kinetics

$$\text{(plastic slip rates)} \qquad \dot{\gamma}^{i} = \dot{\gamma}^{i}\left(\bar{p}^{i}, \bar{\rho}^{i}_{S}, \bar{\eta}^{i}_{S}, \bar{\boldsymbol{\alpha}}, \bar{\boldsymbol{\theta}}, \mathbf{U}^{\mathbf{i}}, T\right), \tag{91}$$

$$\text{(micro} - \text{heterogeneity)} \qquad \mathbf{F}^{\mathbf{i}-1}\dot{\mathbf{F}}^{\mathbf{i}} \equiv \bar{\mathbf{L}}^{\mathbf{i}} = \bar{\mathbf{L}}^{\mathbf{i}}\left(\bar{\mathbf{P}}, \bar{\rho}^{i}_{S}, \bar{\eta}^{i}_{S}, \bar{\boldsymbol{\alpha}}, \bar{\boldsymbol{\theta}}, \mathbf{U}^{\mathbf{i}}, T\right), \tag{92}$$

$$\text{(statistically stored dislocations)} \qquad \dot{\bar{\rho}}^{i}_{S} = \dot{\bar{\rho}}^{i}_{S}\left(\bar{p}^{i}, \bar{\rho}^{i}_{S}, \bar{\eta}^{i}_{S}, \bar{\boldsymbol{\alpha}}, \bar{\boldsymbol{\theta}}, \mathbf{U}^{\mathbf{i}}, T\right), \tag{93}$$

$$\text{(statistically stored disclinations)} \qquad \dot{\bar{\eta}}^{i}_{S} = \dot{\bar{\eta}}^{i}_{S}\left(\bar{p}^{i}, \bar{\rho}^{i}_{S}, \bar{\eta}^{i}_{S}, \bar{\boldsymbol{\alpha}}, \bar{\boldsymbol{\theta}}, \mathbf{U}^{\mathbf{i}}, T\right). \tag{94}$$

Some general comments are now given regarding aspects of our constitutive theory that differ from others in the literature. Our macroscopic ((78)–(80)) and microscopic ((81)–(83)) force balance equations are independent, with the symmetry of the

stress tensor (79) and usual structure for internal energy rate (85) maintained. This is in contrast to the couple stress theory conceived by Fleck, Hutchinson, and co-workers (Fleck and Hutchinson, 1993; Fleck et al., 1994; Gao et al., 1999) that permits a nonsymmetric Cauchy stress. Gurtin (2002, 2004) developed a gradient crystal plasticity theory preserving the symmetry conditions on the macroscopic stress and simultaneously featuring microforce balances on discrete slip systems whereby geometrically necessary dislocations (in terms of both first and second-order spatial gradients of a lattice deformation map $\mathbf{F}^{\mathbf{e}-1}$) may naturally contribute to a backstress on each system. In Gurtin's theory, slip rates perform mechanical work on the boundary of the body and explicitly enter the global energy balance (virtual power principle) from which governing equations are derived. In our theory, the micro-variables do no mechanical work (they are absent in (85)).

In the present work we have postulated the existence of microscopic force balances from the outset, following consideration of balances of higher order moments (54). Alternative approaches for constructing balance relations in higher order theories often employ variational or virtual work principles (e.g., Toupin, 1964; Teodosiu, 1967; Le and Stumpf, 1996a,c; Gurtin, 2002). Our thermodynamic force relations (89) emerge upon division of the total defect density tensors into elastic (storage) and plastic (dissipative) parts, as in Eq. (38). Le and Stumpf (1996a,c) made an alternative prescription, dividing the conjugate defect forces into dissipative and energetic parts, the former associated with evolution laws for defect fluxes and the latter with stress-type balance laws for recoverable elastic deformations and defect densities.

Prior to implementation and subsequent solution of initial-boundary value problems, specific forms of the free energy function (84) and kinetic relations (91)–(94) must be selected for the material under consideration. The framework presented here establishes the need, and serves as a guide, for developing appropriate experiments, both physical and numerical, necessary for simulation of a generalized continuum accounting for the generation, motion, and interaction of dislocation and disclination defects. The dependence of the free energy upon periodic defect distributions can be extracted from homogenization of atomistic solutions, for example (Chung, 2004). A non-convex potential (84) will promote the development of heterogeneous deformation fields in a body subjected to nominally homogeneous initial and boundary conditions, as discussed by example in Appendix A. Note that normalizing length scale parameters or constants (Gao et al., 1999; Regueiro et al., 2002; Al-Rub and Voyiadjis, 2004; Huang et al., 2004) associated with the dislocation and disclination density tensors are expected to enter the free energy and kinetic relations, as these defect densities are not dimensionless.

From the perspective of numerical solution of boundary value problems, Eqs. (68)–(94) are formidable. Consider this framework in comparison to that of standard crystal plasticity (e.g., Asaro, 1983). The additional kinematic unknowns present in the former relative to the latter are $\mathbf{F}^{\mathbf{i}}$ (Eq. (68)) and $\mathbf{Q}$ (Eq. (73)), each having nine independent components. Note that the defect density tensors can be derived directly from $\mathbf{F}^{\mathscr{L}}$ and $\mathbf{Q}$ via (74) and (75). The corresponding additional equations in our framework are kinematic relations (76) (3 equations relating the residual lattice rotation and the disclination density, which in turn is a function of $\mathbf{Q}$ and its spatial

gradients), microforce balances (81) and (82) (a total of 6 equations), and the kinetic equations for $\mathbf{F}^{\mathbf{i}}$ in (92) (9 equations). When geometrically necessary disclinations are absent, $\mathbf{Q} = \mathbf{0}$, $\mathbf{R}^{\mathbf{i}} = \mathbf{1}$, geometrically necessary dislocations are found from curl of the (inverse) lattice deformation gradient via (72)–(74), and satisfaction of the microforce balances is trivially ensured upon proper choice of free energy dependency on dislocations (e.g., a dislocation driving force $\boldsymbol{\sigma}$ proportional to a curl of a tensor field will be divergence-free). For example, a particularly simple, yet illustrative, form for the free energy function (84) in the absence of disclination densities is the following:

$$\tilde{\psi} = \left(\tilde{C}^{e}_{\alpha\beta} - \tilde{g}_{\alpha\beta}\right)\mathbb{C}^{\alpha\beta\chi\delta}\left(\tilde{C}^{e}_{\chi\delta} - \tilde{g}_{\chi\delta}\right) + \tilde{\mu}\ell^{2}\tilde{\alpha}^{(\alpha\beta)}\tilde{g}_{\beta\chi}\tilde{g}_{\alpha\delta}\tilde{\alpha}^{(\delta\chi)} + \tilde{\psi}_{1}\left(V^{i\alpha}_{\ .\beta}\right) + \tilde{\psi}_{2}\left(\tilde{\varepsilon}_{\rho}\right) + \tilde{\psi}_{3}(T), \tag{95}$$

where $\mathbb{C}^{\alpha\beta\chi\delta}$ are temperature-dependent elastic moduli, and where $\tilde{\psi}_1$, $\tilde{\psi}_2$, and $\tilde{\psi}_3$ are functions of their arguments, with $\tilde{\psi}_3$ accounting for the specific heat capacity of the material. Notice that the second term in (95) consists of a quadratic form of the symmetric part of the dislocation density tensor $\tilde{\boldsymbol{\alpha}}$, pre-multiplied by an effective elastic shear modulus $\tilde{\mu}$ and normalized by squared length parameter ℓ. In this case, setting the micro-traction (hyperstress) boundary condition $\bar{\mathbf{t}}_{\boldsymbol{\mu}} = \mathbf{0}$ for the second of (83) in conjunction with the prescription $\mathbf{R}^{\mathbf{i}-1}\dot{\mathbf{R}}^{\mathbf{i}} = \mathbf{0}$ for spin components of rate Eq. (92) leads to the (correct) trivial solution $\mathbf{Q} = \mathbf{0}$ in (72) and $\mathbf{R}^{\mathbf{i}} = \mathbf{1}$ in (76), assuming for initial conditions a defect-free reference lattice. In other words, substituting (95) into (81) and (82) yields the identically satisfied expressions $\sigma^{\bar{\alpha}b}_{\ \ .b} = \tilde{\mu}\ell^{2}\varepsilon^{bcd}F^{\mathscr{L}-1\bar{\alpha}}_{\ \ .d,cb} = 0$ and $\bar{\varepsilon}_{\bar{\alpha}\bar{\beta}\bar{\chi}}F^{\mathscr{L}-1\bar{\beta}}_{\ \ .b}\sigma^{\bar{\chi}b} = J^{e-1}\tilde{\mu}\ell^{2}\bar{\varepsilon}_{\bar{\alpha}\bar{\beta}\bar{\chi}}F^{i-1\bar{\chi}}_{\ \ .\alpha}\tilde{\alpha}^{(\alpha\bar{\beta})}F^{i-1\bar{\beta}}_{\ \ .\beta} = 0$, respectively, written here in Cartesian spatial coordinates. Notice that the defect densities (i.e., higher order deformation gradients) can enter the kinetic relations (91)–(94), effectively rendering these partial differential equations in time and space. Further elaboration upon the role of higher-order traction boundary conditions (83) and their kinematic counterparts is deferred to future work wherein specific free energy and kinetic relations will be developed for plastically deforming crystals containing evolving distributions of dislocations and disclinations.

5. Concluding remarks

A general finite strain theory incorporating dislocation and disclination defects has been introduced, based primarily on volume averaging considerations. Novel features of the kinematic description include a three-term decomposition of the average deformation gradient for a crystalline volume element and an independent micropolar rotation variable associated with incompatible spatial gradients of lattice rotation within the element. The latter may be attributed to misoriented subgrain cells separated by walls of partial disclination dipoles. The micropolar rotations execute independently of the continuum rotations associated with elastic and inelastic components of the deformation gradient, and are intended to capture physics that geometrically necessary dislocations associated with first order gradients of

incompatible elastic or plastic deformations cannot represent alone. For example, these micro-rotations may evolve even under nominally homogeneous applied deformations to single crystals, in contrast to geometrically necessary dislocation theories requiring heterogeneity of deformation at the scale of the crystal to drive the evolution of defects (see the discussion in Ortiz and Repetto, 1999; Ortiz et al., 2000, whose lamination model also intends to represent such effects). Our theory separates the role of incompatibility into contributions from higher order deformation gradients (incorporated primarily in the torsion or geometrically necessary dislocation tensor) and subgranular lattice rotation gradients (incorporated in the curvature or geometrically necessary disclination tensor), although the constitutive equations ultimately dictating their evolution are in general strongly coupled. The kinematic framework has strong ties to geometrically oriented defect field theories of the mid- to late-twentieth century (Bilby et al., 1955; Noll, 1967; Lardner, 1973; Minagawa, 1979; De Wit, 1981), and reduces to a formulation consistent with previous gradient-based dislocation theories of the co-authors (cf. Bammann, 2001; Regueiro et al., 2002; Clayton et al., 2004a) when micropolar rotations and disclinations are excluded. Our theory admits the coupling of applied and residual elastic strain energy densities, arising physically from the bowing of dislocation structures due to applied loads, through the appropriate choice of free energy function (45). Higher order microstresses satisfy balance laws independent of those associated with the macroscopic Cauchy stress, and exhibit a form comparable to classical couple stress theory (Eringen and Claus, 1970; Minagawa, 1979). Kinetic relations are left in a general format applicable to generic metallic crystals. We expect the additional assertion of maximal dissipation rate to serve as an heuristic tool for partitioning dislocation and disclination kinetics. Also required is a more thorough examination of the supplemental boundary conditions (83) associated with the lattice arrangement (cf. Acharya et al., 2004).

The model is expected to capture grain size effects on initial yielding and strain hardening, the former via proper choices of initial conditions for geometrically necessary dislocations and disclinations and their inclusion in the initial slip resistances, the latter via evolution of the crystal defects (cf. Evers et al., 2002) and their incorporation in the viscoplastic flow rule. Since relatively strong lattice rotation gradients are expected in the vicinity of grain boundary regions (Bergugnat, 2002) and may be correlated to measured hardness increases near such boundaries (Soifer et al., 2002), initial conditions on the micro-rotation variable and defect densities should reflect larger initial yield stresses in relatively fine-grained microstructures that exhibit more grain boundary surface area per unit volume than relatively coarse-grained polycrystals. This accords with the premise of a recent paper by Gerberich et al. (2003) in which size effects observed in nano-indentation of metallic crystals and delamination of thin films are shown to scale with characteristic surface-to-volume ratios, as well as the increasing normalized strength with increasing surface-area-to-volume ratios observed in the wire torsion experiments of Fleck et al. (1994). Potential applications of our theory include stages 3 and 4 of plastic deformation at various deformation rates, as fragmentation into cellular structures has been observed in FCC, BCC, and HCP structures at large strains (Seefeldt, 2001), extremely fine-grained

"nanocrystalline" materials exhibiting high grain boundary surface area densities (Benson et al., 2001; Aleksandrov et al., 2002; Valiev et al., 2002), and creep conditions where subgrain formation frequently occurs (Kratochvíl and Orlová, 1990; Kassner and Pérez-Prado, 2000; Seefeldt and Aifantis, 2002).

Acknowledgments

J.D.C. acknowledges support from the Weapons and Materials Research Directorate of the U.S. Army Research Laboratory. D.J.B. is grateful for support of Sandia National Laboratories under U.S. Department of Energy contract no. DE-AC04-94AL85000. D.L.M. acknowledges support of AFOSR (MURI (1606U81) and F49620-01-1-0034), along with the Carter Paden, Jr. Chair in Metals Processing.

Appendix A. Kinematics and kinetics of grain subdivision

Here we illustrate how our framework may be applied to describe evolution of defect substructure observed in ductile (predominantly pure FCC) metals deformed at low homologous temperatures and low strain rates to relatively large total strains (Pantleon, 1996; Hughes et al., 1997, 1998, 2003; Hughes and Hansen, 2000; Hughes, 2001). As shown in Fig. 7(a), typically this substructure consists of nearly equiaxed "cells" with interiors of relatively low defect density, separated by "Incidental Dislocation Boundaries" (IDBs) across which lattice misorientations are generally of the low-angle variety, for example, limited to less than 10° in aluminum and nickel cold-rolled to 100% effective strain (Hughes et al., 2003). With increasing applied strain, the cells tend to organize collectively into bands or "cell blocks", often elongated in shape in a direction depending upon the initial texture and loading conditions. The cell blocks are separated by dislocation walls termed "Geometrically Necessary Boundaries" (GNBs), across which misorientations can reach high-angle magnitudes (i.e., in excess of 15°). Average cell and cell block sizes decrease with increasing applied strain, with the cell block size generally decreasing at a significantly faster rate than the cell size (Hughes et al., 1997). Both GNBs and IDBs are thought to contain mixed populations of redundant (i.e., statistically stored) and non-redundant (i.e.,

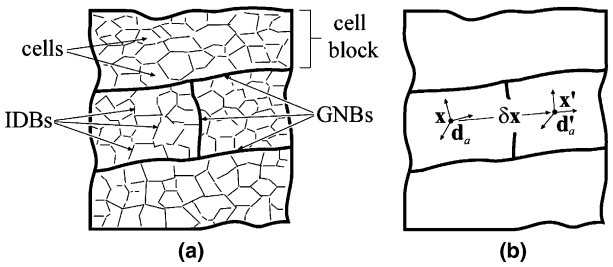

Fig. 7. Dislocation substructure (a) and lattice directors (b) in a deformed single crystal.

geometrically necessary) dislocations (Hughes et al., 2003). It is also noted that other terminology exists for similar defect substructures; for example, Kuhlmann-Wilsdorf and co-workers (Kuhlmann-Wilsdorf et al., 1999) used the term "Deformation Bands" to denote slab-shaped volume elements within which a reduced number of slip systems is active for arbitrary shape changes (i.e., fewer than five systems), with such volume elements delineated by GNBs. However, attention is focused here on the observations, terminology, and hypotheses of Hughes, Hansen, and co-workers detailed in the aforementioned cited references.

In the context our framework, the kinematics of the above defect substructure can be described as follows. Redundant dislocations and disclinations that contribute no net observed misorientation (i.e., no incompatibility) are grouped collectively into the statistically stored dislocation and disclination scalars $\bar{\rho}^i_S$ and $\bar{\eta}^i_S$, respectively. Geometrically necessary dislocations (i.e., the net dislocation tensor $\boldsymbol{\alpha}$) represent the non-redundant defect component corresponding to fluctuations in lattice orientation across the cell boundaries (i.e., IDBs). The micro-rotation variable $\mathbf{Q}$ (in conjunction with associated net disclination density tensor $\boldsymbol{\theta}$) depicts the non-redundant dislocation component of the cell block boundaries (i.e., GNBs). Fractions of dislocations and disclinations that are geometrically necessary may differ, as they represent different features of the microstructure: IDBs and GNBs, respectively.

The general theory developed in Sections 2 and 3 of the present paper places no restrictions on the characteristic spacing or the strength of the physical misorientation boundary to which we attribute a particular type of defect density. For example, we could alternatively allow dislocations to comprise GNBs and disclinations to comprise IDBs, or allow a mixture of defect types to comprise each kind of boundary. Our decision here to model GNBs with the disclination density and IDBs with the dislocation density stems from both convenience and from physical considerations in agreement with models set forth in prior literature (Panin, 1998; Seefeldt, 2001). From the perspective of calibrating the constitutive model to physical observations, it is most convenient to assign one type of defect density (i.e., dislocation or disclination) to one type of boundary (i.e., IDB or GNB) such that material parameters and kinetic relations can be chosen to reflect the corresponding physics, for example average misorientation angles and wall spacings. Following Panin (1998) and Seefeldt (2001), we associate the rotational units that serve to accommodate inelastic deformation and subgranular incompatibility seen at comparatively large strains with disclinations (GNBs), with geometrically necessary dislocations capturing the local misorientations across IDBs arising at a finer length scale. From this standpoint, upon inelastic straining, IDBs (i.e., dislocations) accumulate first, and then later organize into GNBs (i.e., disclination boundaries) at larger applied deformations.

The micro-rotation concept is illustrated in Fig. 7(b) with regard to lattice vectors. Let $\mathbf{x}$ and $\mathbf{x}'$ be spatial coordinates of material points in neighboring cell blocks, with corresponding lattice director vectors $\mathbf{d}_a$ and $\mathbf{d}'_a$. Assume that in elastically unloaded configuration $\bar{b}$, the director triads are parallel, i.e.,

$$\bar{\mathbf{d}}_{\bar{\alpha}} = \bar{\mathbf{d}}'_{\bar{\alpha}}. \tag{A.1}$$

Let $\mathbf{F}^{\mathscr{L}}$ and $\mathbf{F}^{\mathscr{L}\prime}$ denote the local lattice deformations at $\mathbf{x}$ and $\mathbf{x}'$, respectively. Multiplying both sides of (A.1) by $\mathbf{F}^{\mathscr{L}\prime-1}$, we arrive at the following relationship between $\mathbf{d}_a$ and $\mathbf{d}'_a$:

$$\mathbf{d}'_a = \left(\left(F^{\mathscr{L}-1}\right)^{\bar{\alpha}}_{.a} + \frac{\left(F^{\mathscr{L}\prime-1}\right)^{\bar{\alpha}}_{.a} - \left(F^{\mathscr{L}-1}\right)^{\bar{\alpha}}_{.a}}{(x'^c - x^c)}(x'^c - x^c) \right) \left(F^{\mathscr{L}}\right)^{b}_{.\bar{\alpha}} \mathbf{d}_b. \tag{A.2}$$

We also have, from (19) and the assertion of parallel transport (i.e., $\nabla_b \mathbf{d}_a = 0$),

$$\mathbf{d}'_a = \left(\left(F^{\mathscr{L}-1}\right)^{\bar{\alpha}}_{.a} + \left(F^{\mathscr{L}-1}\right)^{\bar{\alpha}}_{.a,c}\delta x^c + \left(F^{\mathscr{L}-1}\right)^{\bar{\alpha}}_{.d} Q^{.d}_{ca}\delta x^c \right) F^{\mathscr{L}b}_{.\bar{\alpha}} \mathbf{d}_b, \tag{A.3}$$

where $\delta x^c \equiv x'^c - x^c$ and $\mathbf{d}'_a - \mathbf{d}_a \approx \mathbf{d}_{a,b}\delta x^b$. We thus see, upon comparing (A.2) and (A.3), that $\mathbf{Q}$ represents the "error" in the capability for the first spatial gradient of $\mathbf{F}^{\mathscr{L}-1}$ to capture the absolute change in the lattice directors over the small distance δx^c, i.e.,

$$Q^{.d}_{ca} = F^{\mathscr{L}d}_{.\bar{\alpha}} \left(\frac{\left(F^{\mathscr{L}\prime-1}\right)^{\bar{\alpha}}_{.a} - \left(F^{\mathscr{L}-1}\right)^{\bar{\alpha}}_{.a}}{(x'^c - x^c)} - \left(F^{\mathscr{L}-1}\right)^{\bar{\alpha}}_{.a,c} \right). \tag{A.4}$$

Equivalently, one can think of $\mathbf{Q}$ as representative of the effects of higher than first order gradients of the lattice deformation $\mathbf{F}^{\mathscr{L}}$ on the spatial variation of the lattice directors. In typical higher-order gradient crystal plasticity theories from the recent literature (cf. Nagdhi and Srinivasa, 1993; Le and Stumpf, 1996a; Shizawa and Zbib, 1999; Acharya and Bassani, 2000; Bammann, 2001; Regueiro et al., 2002; Garikipati, 2003; Clayton et al., 2004a), only the first order gradient of the elastic or plastic deformation (e.g., only the first gradient of $\mathbf{F^e}$ or $\mathbf{F^p}$ when the usual decomposition $\mathbf{F} = \mathbf{F^e F^p}$ is implemented) influences the material response, through its manifestation in the geometrically necessary dislocation density tensor. However, by including the micro-rotation variable $\mathbf{Q}$, the potentially nonlinear variation in lattice directors (i.e., higher than first order gradients of $\mathbf{F}^{\mathscr{L}}$) between neighboring material points is captured in the response in the present theory. This nonlinearity is manifested in our GND density tensor and in our disclination density tensor through $\mathbf{Q}$ term and its spatial gradient, respectively (see Eqs. (23), (25) and (29)). Physically, this nonlinearity can be attributed to the superposition of lattice rotations across GNBs between cell blocks with the rotations across IDBs between the cells. Under the assumption that the misorientations across the GNBs remain small, the disclination density tensor simplifies to the linear approximation

$$4\theta^{gd} \equiv \varepsilon^{gba}\varepsilon^{dce} R_{abce} \approx 2\varepsilon^{gba}\varepsilon^{dce}\partial_{[c} Q_{e][ba]} = 2\varepsilon^{gba}\varepsilon^{dce} Q_{eba,c}. \tag{A.5}$$

We now consider kinetics briefly in the context of the experimental data reported by Hughes et al. (1997, 1998, 2003). Evolution equations applicable in this context should reflect the following physical phenomena:

- Characteristic scaling of misorientation *distributions* for IDBs and GNBs.
- Characteristic scaling of size *distributions* for cells and cell blocks.

- Increase in *average* IDB misorientation proportional to $(\bar{\varepsilon}^p)^{1/2}$, and increase in average GNB misorientation proportional to $(\bar{\varepsilon}^p)^{2/3}$, where $\bar{\varepsilon}^p$ is the effective macroscopic plastic strain.
- Reduction in *average* cell and cell block sizes proportional to $(\bar{\varepsilon}^p)^{-1/2}$ and $(\bar{\varepsilon}^p)^{-2/3}$, respectively.

Furthermore, the final microstructural configuration attained in a simulation of material behavior should reflect observations regarding cellular misorientation and size distributions, and can be chosen to reflect a path of minimum stored residual elastic energy (i.e., maximum dissipation). In other words, for the same boundary conditions, more total dissipation over the deformation history is expected for attainment of a low-energy configuration consisting of collectively organized geometrically necessary and statistically stored defects than would be expected for attainment of a plastically homogeneously deforming crystal containing a distribution of redundant (i.e., statistically stored) defects alone. Moreover, greater total dissipation is expected over the deformation history for attainment of the actual configuration of defects than for any other candidate distribution of these defects. We recognize that construction of specific kinetic relations capturing the above listed features of the response within the context of our general theory is a non-trivial task, one that will be undertaken more rigorously in forthcoming works.

Our framework admits the possibility of evolution of a heterogeneous deformation gradient field in conjunction with affine boundary conditions based upon energetic arguments. Rather than specify deterministically the slip rates $\dot{\gamma}^i$ as implied in Section 3, we may instead re-write (57) as incremental relations

$$d\gamma^i = d\gamma^i\left(\bar{p}^i, \bar{\rho}^i_S, \bar{\eta}^i_S, \bar{\boldsymbol{\alpha}}, \bar{\boldsymbol{\theta}}, \mathbf{U}^{\mathbf{i}}, T, \tilde{\Psi}(t)\right), \tag{A.6}$$

where we have added dependence upon the global free energy of the entire crystal or polycrystal (i.e., entire domain V of the specific boundary value problem), with this energy denoted by $\tilde{\Psi} \equiv \int \tilde{\psi} dV$. Conceptually, one may predict the evolution of the slip increments (A.6) by sequential minimization of $\tilde{\Psi}$, subject to constraints imposed by the other dependent variables and physical observations (Ortiz et al., 2000). A non-convex potential $\tilde{\psi}$ may lead to lack of existence of minimum energy configurations corresponding to a homogeneous deformation gradient field; instead, such configurations may be reached in the limit of further refined microstructures (e.g., heterogeneous deformation gradient fields and slip rates within the domain), as explained thoroughly in prior literature (cf. Ball and James, 1987; Ortiz and Repetto, 1999; Carstensen et al., 2002).

To illustrate how one might achieve a non-convex energy potential in the context of our theory, we present an idealized 1D problem. Neglecting for this simple example the contributions of geometrically necessary defects, and assuming fixed temperature, consider a non-recoverable free energy $\tilde{\psi}^S$ depending quadratically upon the statistically stored defect densities:

$$\tilde{\psi}^S = \frac{1}{2}\mu\left[\left(c_\rho \tilde{\varepsilon}_\rho\right)^4 + \left(c_\eta \tilde{\varepsilon}_\eta\right)^4\right] = \frac{1}{2}\mu\left[\left(bc_\rho\right)^4 \tilde{\rho}_S^2 + \left(r\omega c_\eta\right)^4 \tilde{\eta}_S^2\right], \tag{A.7}$$

where c_ρ and c_η are dimensionless parameters. We let γ denote the local inelastic strain in the crystal, which we assume evolves monotonically, enabling its use as a parameter in the kinetics equations in lieu of time. Assume that the evolution equations (61), mapped to configuration $\tilde{b}$ and parameterized in terms of strain, are of the form

$$\frac{\partial \tilde{\rho}_S}{\partial \gamma} = A - B\tilde{\eta}_S, \quad \frac{\partial \tilde{\eta}_S}{\partial \gamma} = C, \tag{A.8}$$

where A, B, and C are positive material-dependent constants of the appropriate dimensions. The first of (A.8) states that dislocations accumulate at a constant rate minus a term representing their trapping and accumulation at disclination boundaries. The second simply denotes a constant rate of increase in disclination density with strain. We remark that Eqs. (A.7) and (A.8), while perhaps physically plausible, present a drastically simplified rendition of the general theory and are introduced here for illustrative purposes only. They are not necessarily representative of the behavior of any particular material. Assuming initial conditions $\tilde{\rho}_S = \tilde{\eta}_S = 0$ at $\gamma = 0$, the solution of differential equations (A.8) is found trivially as

$$\tilde{\rho}_S = A\gamma - \frac{BC}{2}\gamma^2, \quad \tilde{\eta}_S = C\gamma. \tag{A.9}$$

Substituting (A.9) into (A.7) then returns the stored energy as a function of γ, i.e.,

$$\tilde{\psi}^S = \frac{1}{2}\mu\left[(bc_\rho)^4\left(A^2\gamma^2 - ABC\gamma^3 - \left(\frac{BC}{2}\right)^2\gamma^4\right) + (r\omega c_\eta)^4 C^2\gamma^2\right], \tag{A.10}$$

with its second derivative found as

$$\frac{\partial^2 \tilde{\psi}^S}{\partial \gamma^2} = \frac{1}{2}\mu\left[(bc_\rho)^4\left(2A^2 - 6ABC\gamma - 12\left(\frac{BC}{2}\right)^2\gamma^2\right) + 2(r\omega c_\eta)^4 C^2\right], \tag{A.11}$$

leading to the conclusion that $\tilde{\psi}^S(\gamma)$ is strictly convex when

$$A^2 + \left(\frac{r\omega c_\eta}{bc_\rho}\right)^4 C^2 > 3ABC\gamma + 6\left(\frac{BC}{2}\right)^2\gamma^2. \tag{A.12}$$

Inequality (A.12) is satisfied when $C = 0$ (no disclinations) or $A = B = 0$ (no dislocations), but is not satisfied in the general case for all $\gamma > 0$ and $B \neq 0$. Thus we see from this simple example that even though the stored energy is convex (quadratic in this case) in each individual defect density variable, its cross-convexity is not ensured due to the coupling between the evolution equations, when $B \neq 0$. Should the evolution of local inelastic strain γ be dictated by energy minimization principles (cf. Ortiz et al., 2000), the non-convexity of $\tilde{\psi}^S$ would be expected to promote a spatially heterogeneous distribution of this strain and spatial patterning of underlying dislocation and disclination densities.

References

Acharya, A., Bassani, J.L., 2000. Lattice incompatibility and a gradient theory of crystal plasticity. J. Mech. Phys. Solids 48, 1565–1595.

Acharya, A., 2001. A model of crystal plasticity based on the theory of continuously distributed dislocations. J. Mech. Phys. Solids 49, 761–785.

Acharya, A., 2003. Driving forces and boundary conditions in continuum dislocation mechanics. Proc. R. Soc. Lond. A 459, 1343–1363.

Acharya, A., Tang, H., Saigal, S., Bassani, J.L., 2004. On boundary conditions and plastic strain-gradient discontinuity in lower-order gradient plasticity. J. Mech. Phys. Solids 52, 1793–1826.

Aifantis, E.C., 1987. The physics of plastic deformation. Int. J. Plasticity 3, 211–247.

Aleksandrov, I.V., Raab, G.I., Shestakova, L.O., Kil'mametov, A.R., Valiev, R.Z., 2002. Refinement of tungsten microstructure by severe plastic deformation. Phys. Met. Metall. 93, 493–500.

Al-Rub, R.K.A., Voyiadjis, G.Z., 2004. Analytical and experimental determination of the material intrinsic length scale of strain gradient plasticity theory from micro- and nano-indentation. Int. J. Plasticity 20, 1139–1182.

Amari, S., 1981. Dualistic theory of non-Riemannian material manifolds. Int. J. Eng. Sci. 19, 1581–1594.

Anthony, K.H., 1969. Nonmetric connexions, quasidislocations, and quasidisclinations. A contribution to the theory of nonmechanical stresses in crystals. Fundamental Aspects of Dislocation Theory. NBS Publication 317. U.S. Government Printing Office, Gaithersburg, MD.

Argon, A.S., Takeuchi, S., 1981. Internal stresses in power-law creep. Acta Metall. 29, 1877–1884.

Asaro, R.J., 1983. Crystal plasticity. J. Appl. Mech. 50, 921–934.

Ashby, M.F., 1970. The deformation of plastically non-homogeneous materials. Philos. Mag. 21, 399–424.

Arsenlis, A., Parks, D.M., Becker, R., Bulatov, V.V., 2004. On the evolution of crystallographic dislocation density in non-homogeneously deforming crystals. J. Mech. Phys. Solids 52 (6), 1213–1246.

Ball, J.M., James, R.D., 1987. Fine phase mixtures as minimizers of energy. Arch. Rat. Mech. Anal. 100, 13–52.

Bammann, D.J., 2001. A model of crystal plasticity containing a natural length scale. Mater. Sci. Eng. A 309–310, 406–410.

Bammann, D.J., Aifantis, E.C., 1982. On a proposal for a continuum with microstructure. Acta Mech. 45, 91–121.

Barton, N.R., Dawson, P.R., 2001. A methodology for determining average lattice orientation and its application to the characterization of grain substructure. Metal. Mater. Trans. A 32, 1967–1975.

Benson, D.J., Fu, H.-H., Meyers, M.A., 2001. On the effect of grain size on yield stress: extension into nanocrystalline domain. Mater. Sci. Eng. A 319–321, 854–861.

Bergugnat, J.-B., 2002. Strain and lattice rotation fields of deformed polycrystals. M.S. Thesis, Georgia Institute of Technology, Atlanta, GA, USA.

Berveiller, M., Muller, D., Kratochvíl, J., 1993. Nonlocal versus local elastoplastic behavior of heterogeneous materials. Int. J. Plasticity 9, 633–652.

Bhattacharya, K., 1991. Wedge-like microstructure in martensites. Acta Metall. Mater. 39, 2431–2444.

Bilby, B.A., Bullough, R., Smith, E., 1955. Continuous distributions of dislocations: a new application of the methods of non-Riemannian geometry. Proc. R. Soc. Lond. A 231, 263–273.

Bilby, B.A., Gardner, L.R.T., Stroh, A.N., 1957. Continuous distributions of dislocations and the theory of plasticityProceedings of the 9th International Congress on Applied Mechanics, Bruxelles, 1956, vol. 8. Université de Bruxelles, pp. 35–44.

Bollmann, W., 1991. The stress field of a model triple line disclination. Mater. Sci. Eng. A 136, 1–7.

Butler, G.C., McDowell, D.L., 1998. Polycrystal constraint and grain subdivision. Int. J. Plasticity 14, 703–717.

Butler, G.C., Stock, S.R., McDowell, D.L., 2000. X-ray microbeam diffraction studies of large strain dislocation substructure formation in OFHC copper. Key Eng. Mater. 177–180, 165–170.

Capolungo, L., Jochum, C., Cherkaoui, M., Qu, J., 2005. Homogenization method for strength and inelastic behavior of nanocrystalline materials. Int. J. Plasticity 21, 67–82.

Carstensen, C., Hackl, K., Mielke, A., 2002. Non-convex potentials and microstructures in finite-strain plasticity. Proc. R. Soc. Lond. A 458, 299–317.

Cermelli, P., Fried, E., 2002. The evolution equation for a disclination in a nematic liquid crystal. Proc. R. Soc. Lond. A 458, 1–20.

Chung, P.W., 2004. Computational method for atomistic homogenization of nanopatterned point defect structures. Int. J. Numer. Meth. Eng. 60, 833–859.

Clayton, J.D., McDowell, D.L., 2003. A multiscale multiplicative decomposition for elastoplasticity of polycrystals. Int. J. Plasticity 19, 1401–1444.

Clayton, J.D., McDowell, D.L., Bammann, D.J., 2004a. A multiscale gradient theory for elastoviscoplasticity of single crystals. Int. J. Eng. Sci. 42, 427–457.

Clayton, J.D., Bammann, D.J., McDowell, D.L., 2004b. Anholonomic configuration spaces and metric tensors in finite elastoplastcity. Int. J. Non-linear Mech. 39, 1039–1049.

Coleman, B.D., Gurtin, M.E., 1967. Thermodynamics with internal state variables. J. Chem. Phys. 17, 597–613.

Coleman, B.D., Noll, W., 1963. The thermodynamics of elastic materials with heat conduction and viscosity. Arch. Rat. Mech. Anal. 13, 167–178.

Cosserat, E., Cosserat, F., 1909. Théorie Des Corps Déformables. Hermann, Paris.

Das, E.S.P., Marcinkowski, M.J., Armstrong, R.W., De Wit, R.W., 1973. The movement of Volterra disclinations and the associated mechanical forces. Philos. Mag. 27, 369–391.

De Wit, R., 1971. Relation between dislocations and disclinations. J. Appl. Phys. 42, 3304–3308.

De Wit, R., 1973. Continuous distribution of disclination loops. Phys. Stat. Sol. A 18, 669–681.

De Wit, R., 1981. A view of the relation between the continuum theory of lattice defects and non-Euclidean geometry in the linear approximation. Int. J. Eng. Sci. 19, 1475–1506.

Dillon, O.W., Kratochvíl, J., 1970. A strain gradient theory of plasticity. Int. J. Solid Struct. 6, 1513–1533.

Dillon, O.W., Perzyna, P., 1972. A gradient theory of materials with memory and internal changes. Arch. Mech. 24, 727–747.

Eisenhart, L.P., 1926. Riemannian Geometry. Princeton University Press, Princeton, NJ.

Eringen, A.C., 1972. Nonlocal polar elastic continua. Int. J. Eng. Sci. 10, 1–16.

Eringen, J.A., Claus Jr., W.D., 1970. A micromorphic approach to dislocation theory and its relation to several existing theories. In: de Wit, R., Bullough, R. (Eds.), Fundamental Aspects of Dislocation Theory. U.S. Government Printing Office, Gaithersburg, MD, vol. 2, pp. 1023–1040.

Eshelby, J.D., 1951. The force on an elastic singularity. Phil. Trans. R. Soc. Lond. A 244, 87–111.

Eshelby, J.D., 1975. The elastic energy-momentum tensor. J. Elasticity 5, 321–335.

Evers, L.P., Parks, D.M., Brekelmans, W.A.M., Geers, M.G.D., 2002. Crystal plasticity model with enhanced hardening by geometrically necessary dislocation accumulation. J. Mech. Phys. Solids 50, 2403–2424.

Fleck, N.A., Hutchinson, J.W., 1993. A phenomenological theory for strain gradient effects in plasticity. J. Mech. Phys. Solids 41, 1825–1857.

Fleck, N.A., Muller, G.M., Ashby, M.F., Hutchinson, J.W., 1994. Strain gradient plasticity: theory and experiments. Acta Metall. Mater. 42, 475–487.

Fox, N., 1968. On the continuum theory of dislocations and plasticity. Quart. J. Mech. Appl. Math. 21, 67–75.

Frank, F.C., 1958. On the theory of liquid crystals. Disc. Faraday Soc. 25, 19–28.

Fu, H.-H., Benson, D.J., Myers, M.A., 2001. Analytical and computational description of effect of grain size on yield stress of metals. Acta Mater. 49, 2567–2582.

Gao, H., Huang, Y., Nix, W.D., Hutchinson, J.W., 1999. Mechanism-based strain gradient plasticity – I. Theory. J. Mech. Phys. Solids 47, 1239–1263.

Garikipati, K., 2003. Couple stresses in crystalline solids: origins from plastic slip gradients, dislocation core distortions, and three-body interatomic potentials. J. Mech. Phys. Solids 51, 1189–1214.

Gerberich, W.W., Jungk, J.M., Li, M., Volinsky, A.A., Hoehn, J.W., Yoder, K., 2003. Length scales for the fracture of nanostructures. Int. J. Fract. 119/120, 387–405.

Gertsman, V.Y., Nazarov, A.A., Romanov, A.E., Valiev, R.Z., Vladimirov, V.I., 1989. Disclination-structural unit model of grain boundaries. Philos. Mag. A 59, 1113–1118.

Gibeling, J.C., Nix, W.D., 1980. A numerical study of long range internal stresses associated with subgrain boundaries. Acta Metall. 28, 1743–1752.
Groma, I., Csikor, F.F., Zaiser, M., 2003. Spatial correlations and higher-order gradient terms in a continuum description of dislocation dynamics. Acta Mater. 51, 1271–1281.
Green, A.E., Rivlin, R.S., 1964. Simple forces and stress multipoles. Arch. Rat. Mech. Anal. 16, 325–353.
Günther, W., 1958. Zur Statik und Kinematik des Cosseratschen Kontinuums. Abh. Braunschweigische Wiss. Ges. 10, 195.
Gurtin, M.E., 2000. On the plasticity of single crystals: free energy, microforces, plastic strain gradients. J. Mech. Phys. Solids 48, 989–1036.
Gurtin, M.E., 2002. A gradient theory of single-crystal viscoplasticity that accounts for geometrically necessary dislocations. J. Mech. Phys. Solids 50, 5–32.
Gurtin, M.E., 2004. On a framework for small-deformation viscoplasticity: free energy, microforces, strain gradients. Int. J. Plasticity 19, 47–90.
Hall, E.O., 1951. The deformation and aging of mild steel. Part III: discussion of results. Phys. Soc. Lond. Proc. 64, 747–753.
Hartley, C.S., 1975. Linear force and dislocation multipoles in anisotropic elasticity. J. Appl. Phys. 46, 1008–1012.
Hartley, C.S., 2003. A method for linking thermally activated dislocation mechanisms of yielding with continuum plasticity theory. Philos. Mag. 83, 3783–3808.
Hill, R., 1972. On constitutive macro-variables for heterogeneous solids at finite strain. Proc. R. Soc. Lond. A 326, 131–147.
Holt, D.L., 1970. Dislocation cell formation in metals. J. Appl. Phys. 41, 3197–3201.
Horstemeyer, M.F., 1995. Physically based models for deformation induced anisotropy. Dissertation, Georgia Institute of Technology, Atlanta, GA.
Horstemeyer, M.F., McDowell, D.L., 1998. Modeling effects of dislocation substructure in polycrystal elastoviscoplasticity. Mech. Mater. 27, 145–163.
Horstemeyer, M.F., McDowell, D.L., McGinty, R.D., 1999. Design of experiments for constitutive model selection: application to polycrystal elastoviscoplasticity. Mod. Simul. Mater. Sci. Eng. 7, 253–273.
Huang, Y., Qu, S., Hwang, K.C., Li, M., Gao, H., 2004. A conventional theory of mechanism-based strain gradient plasticity. Int. J. Plasticity 20, 753–782.
Hughes, D.A., 2001. Microstructure evolution, slip patterns, and flow stress. Mater. Sci. Eng. A 319–321, 46–54.
Hughes, D.A., Chrzan, D.C., Liu, Q., Hansen, N., 1998. Scaling of misorientation angle distributions. Phys. Rev. Lett. 81, 4664–4667.
Hughes, D.A., Hansen, N., 2000. Microstructure and strength of nickel at large strains. Acta Mater. 48, 2985–3004.
Hughes, D.A., Liu, Q., Chrzan, D.C., Hansen, N., 1997. Scaling of microstructural parameters: misorientations of deformation induced boundaries. Acta Mater. 45, 105–112.
Hughes, D.A., Hansen, N., Bammann, D.J., 2003. Geometrically necessary boundaries, incidental dislocation boundaries, and geometrically necessary dislocations. Scr. Mater. 48, 147–153.
Kassner, M.E., Pérez-Prado, M.-T., 2000. Five power-law creep in single phase metals and alloys. Prog. Mater. Sci. 45, 1–102.
Kassner, M.E., Pérez-Prado, M.T., Long, M., Vecchio, K.S., 2002. Dislocation microstructure and internal-stress measurements by convergent-beam electron diffraction on creep-deformed Cu and Al. Metall. Mater. Trans. A 33, 311–317.
Kondo, K., 1964. On the analytical and physical foundations of the theory of dislocations and yielding by the differential geometry of continua. Int. J. Eng. Sci. 2, 219–251.
Konstantinidis, D.A., Aifantis, E.C., 1998. On the "anomalous" hardness of nanocrystalline materials. Nano Mater. 10, 1111–1118.
Kossecka, E., de Wit, R., 1977. Disclination kinematics. Arch. Mech. 29, 633–651.
Kratochvíl, J., 1971. Finite-strain theory of crystalline elastic–inelastic materials. J. Appl. Phys. 42, 1104–1108.

Kratochvíl, J., 1972. Finite-strain theory of inelastic behavior of crystalline solids. In: Sawzcuk, A. (Ed.), Foundations of Plasticity. Noordhoff, Leyder, Warsaw, pp. 401–415.
Kratochvíl, J., Orlová, A., 1990. Instability origin of dislocation substructure. Philos. Mag. A 61, 281–290.
Kröner, E., 1960. Allgemeine kontinuumstheorie der versetzungen und eigenspannungen. Arch. Rat. Mech. Anal. 4, 273–334.
Kröner, E., 1963. On the physical reality of torque stresses in continuum mechanics. Int. J. Eng. Sci. 1, 261–278.
Kröner, E., 1973. The rheological behaviour of metals. Rheol. Acta 12, 374–392.
Kröner, E., 1983. Field theory of defects in Bravais crystals. In: Paidar, V., Lejček, L. (Eds.), The Structure and Properties of Crystal Defects. Elsevier, Amsterdam, pp. 357–369.
Kröner, E., Lagoudas, D.C., 1992. Gauge theory with disclinations. Int. J. Eng. Sci. 30, 47–53.
Kuhlmann-Wilsdorf, D., 1999. The theory of dislocation-based crystal plasticity. Philos. Mag. A 79, 955–1008.
Kuhlmann-Wilsdorf, D., Kulkarni, S.S., Moore, J.T., Starke, E.A., 1999. Deformation bands, the LEDS theory, and their importance in texture development: part I. Previous evidence and new observations. Met. Mater. Trans. A 30, 2491–2501.
Lardner, R.W., 1969. Dislocation dynamics and the theory of the plasticity of single crystals. Z. Agnew. Math. Phys. 20, 514–529.
Lardner, R.W., 1973. Foundations of the theory of disclinations. Arch. Mech. 25, 911–922.
Lardner, R.W., 1974. Mathematical Theory of Dislocations and Fracture. University of Toronto Press, Great Britain.
Lazar, M., Maugin, G.A., 2004. Defects in gradient micropolar elasticity – II: edge dislocation and wedge disclination. J. Mech. Phys. Solids 52, 2285–2307.
Le, K.C., Schutte, H., Stumpf, H., 1998. Dissipative driving force in ductile crystals and the strain localization phenomenon. Int. J. Plasticity 14, 1109–1131.
Le, K.C., Stumpf, H., 1996a. Nonlinear continuum theory of dislocations. Int. J. Eng. Sci. 34, 339–358.
Le, K.C., Stumpf, H., 1996b. On the determination of the crystal reference in nonlinear continuum theory of dislocations. Proc. R. Soc. Lond. A 452, 359–371.
Le, K.C., Stumpf, H., 1996c. A model of elastoplastic bodies with continuously distributed dislocations. Int. J. Plasticity 12, 611–627.
Lee, E.H., Liu, D.T., 1967. Elastic–plastic theory with application to plane-wave analysis. J. Appl. Phys. 38, 19–27.
Leffers, T., 1994. Lattice rotations during plastic deformation with grain subdivision. Mater. Sci. Forum 157–162, 1815–1820.
Leffers, T., 2001. A model for rolling deformation with grain subdivision. Part I: The initial stage. Int. J. Plasticity 17, 469–489.
Li, J.C.M., 1960. Some elastic properties of an edge dislocation wall. Acta Metall. 8, 563–574.
Li, J.C.M., 1972. Disclination model of high angle grain boundaries. Surf. Sci. 31, 12–26.
Li, J.C.M., Gilman, J.T., 1970. Disclination loops in polymers. J. Appl. Phys. 41, 4248–4256.
Lion, A., 2000. Constitutive modelling in finite thermoviscoplasticity: a physical approach based on nonlinear rheological models. Int. J. Plasticity 16, 469–494.
Makarov, P.V., Smolin, I.Y., Prokopinsky, I.P., Stefanov, Y.P., 1999. Modeling of development of localized plastic deformation and prefracture stage in mesovolumes of heterogeneous media. Int. J. Fracture 100, 121–131.
Malvern, L.E., 1969. Introduction to the Mechanics of a Continuous Medium. Prentice-Hall, Englewood Cliffs, NJ.
Mandel, J., 1973. Equations constitutives et directeurs dans les milieux plastiques et viscoplastiques. Int. J. Solid Struct. 9, 725–740.
Mandel, J., 1974. Thermodynamics and plasticity. In: Delgado, J.J., et al. (Eds.), Foundations of Continuum Thermodynamics. Macmillan, New York, pp. 283–304.
Marcinkowski, M.J., 1990. Inter-relationships between dislcinations, surface dislocations, and grain boundaries. Philos. Mag. Lett. 62, 19–23.

Marsden, J.E., Hughes, T.J.R., 1983. Mathematical Foundations of Elasticity. Dover, New York.
Maugin, G.A., 1993. Material Inhomogeneities in Elasticity. Chapman & Hall, London.
Maugin, G.A., 1994. Eshelby stress in elastoplasticity and ductile fracture. Int. J. Plasticity 10, 393–408.
Menzel, A., Steinmann, P., 2000. On the continuum formulation of higher gradient plasticity for single and polycrystals. J. Mech. Phys. Solids 48, 1777–1796.
Meyers, M.A., Ashworth, E., 1982. A model for the effect of grain size on the yield stress of metals. Philos. Mag. A 46, 737–759.
Minagawa, S., 1977. Elastic fields of dislocations and disclinations in an isotropic micropolar continuum. Lett. Appl. Eng. Sci. 5, 85–94.
Minagawa, S., 1979. A non-Riemannian geometrical theory of imperfections in a Cosserat continuum. Arch. Mech. 31, 783–792.
Minagawa, S., 1981. Stress functions and stress function spaces of non-metric connection for 3-dimensional micropolar elastostatics. Int. J. Eng. Sci. 19, 1705–1710.
Mughrabi, H., 1983. Dislocation wall and cell structures and long-range internal stresses in deformed metal crystals. Acta Metall. 31, 1367–1379.
Mughrabi, H., 1988. Dislocation clustering and long-range internal stresses in monotonically and cyclically deformed metal crystals. Rev. Phys. Appl. 23, 367–379.
Mughrabi, H., 2001. On the role of strain gradients and long-range internal stresses in the composite model of crystal plasticity. Mater. Sci. Eng. A 317, 171–180.
Müllner, P., Romanov, A.E., 1994. Between dislocation and disclination models for twins. Scr. Metall. Mater. 31, 1657–1662.
Mura, T., 1982. Micromechanics of Defects in Solids, first ed. Nijhoff, Dordrecht.
Nabarro, F.R.N., 1967. Theory of Crystal Dislocations. Oxford University Press, London.
Nagdhi, P.M., Srinivasa, A.R., 1993. A dynamic theory of structured solids. I. Basic developments. Philos. Trans. R. Soc. Lond. A 345, 425–458.
Nazarov, A.A., Shenderova, O.A., Brenner, D.W., 2000. Elastic models of symmetrical ⟨0 0 1⟩ and ⟨0 1 1⟩ tilt grain boundaries in diamond. Phys. Rev. B 61, 928–936.
Nazarov, A.A., Romanov, A.E., 1989. On the average misorientation angle of general tilt boundaries. Phil. Mag. Lett. 60, 187–193.
Nazarov, A.A., Romanov, A.E., Valiev, R.Z., 1993. On the structure, stress fields, and energy of nonequilibrium grain boundaries. Acta Metall. Mater. 41, 1033–1040.
Nemat-Nasser, S., 1999. Averaging theorems in finite deformation plasticity. Mech. Mater. 31, 493–523.
Noll, W., 1967. Materially uniform simple bodies with inhomogeneities. Arch. Rat. Mech. Anal. 27, 1–32.
Nye, J.F., 1953. Some geometrical relations in dislocated crystals. Acta Metall. 1, 153–162.
Nye, J.F., 1957. Physical Properties of Crystals: Their Representation by Tensors and Matrices. Clarendon Press, Oxford.
Orowan, E., 1940. Problems of plastic gliding. Proc. Phys. Soc. 52, 8–22.
Ortiz, M., Repetto, E.A., 1999. Nonconvex energy minimization and dislocation structures in ductile single crystals. J. Mech. Phys. Solids 47, 397–462.
Ortiz, M., Repetto, E.A., Stainier, L., 2000. A theory of subgrain dislocation structures. J. Mech. Phys. Solids 48, 2077–2114.
Panin, V.E., 1998. Overview on mesomechanics of plastic deformation and fracture of solids. Theor. Appl. Fract. Mech. 30, 1–11.
Pantleon, W., 1996. On the distribution function of disorientations in dislocation cell structures. Scr. Mater. 35, 511–515.
Pęcherski, R.B., 1983. Relation of microscopic observations to constitutive modelling for advanced deformations and fracture initiation of viscoplastic materials. Arch. Mech. 35, 257–277.
Pęcherski, R.B., 1985. Discussion of sufficient condition for plastic flow localization. Eng. Fract. Mech. 21, 767–779.
Peeters, B., Seefeldt, M., Van Houtte, P., Aernoudt, E., 2001. Taylor ambiguity in BCC polycrystals: a non-problem if substructural anisotropy is considered. Scr. Mater. 45, 1349–1356.
Petch, N.J., 1953. The cleavage strength of polycrystals. J. Iron Steel Inst. 174, 25–28.

Regueiro, R.A., Bammann, D.J., Marin, E.B., Garikipati, K., 2002. A nonlocal phenomenological anisotropic finite deformation plasticity model accounting for dislocation defects. J. Eng. Mater. Tech. 124, 380–387.

Rice, J.R., 1971. Inelastic constitutive relations for solids: an internal-variable theory and its application to metal plasticity. J. Mech. Phys. Solids 19, 433–455.

Romanov, A.E., 1993. Screened disclinations in solids. Mater. Sci. Eng. A 164, 58–68.

Rybin, V.V., Zisman, A.A., Zolotorevsky, N.Y., 1993. Junction disclinations in plastically deformed crystals. Acta Metall. Mater. 41, 2211–2217.

Scheidler, M., Wright, T.W., 2001. A continuum framework for finite viscoplasticity. Int. J. Plasticity 17, 1033–1085.

Schouten, J.A., 1954. Ricci Calculus, second ed. Springer, Berlin.

Sedláček, R., Kratochvíl, J., Blum, W., 2001. Deformation induced misorientations: initial stage of subgrain formation as a plastic instability. Phys. Stat. Sol. (a) 186, 1–16.

Seefeldt, M., 2001. Disclinations in large-strain plastic deformation and work-hardening. Rev. Adv. Mater. Sci. 2, 44–79.

Seefeldt, M., Aifantis, E.C., 2002. Disclination patterning under steady-state creep at intermediate temperatures. Solid State Phenomena 87, 221–226.

Seefeldt, M., Delannay, L., Peeters, B., Aernoudt, E., Van Houtte, P., 2001a. Modelling the initial stage of grain subdivision with the help of a coupled substructure and texture evolution algorithm. Acta Mater. 49, 2129–2143.

Seefeldt, M., Delannay, L., Peeters, B., Kalidindi, S.R., Van Houtte, P., 2001b. A disclination-based model for grain subdivision. Mater. Sci. Eng. A 319–321, 192–196.

Seefeldt, M., Klimanek, P., 1997. Interpretation of plastic deformation by means of dislocation–disclination reaction kinetics. Mater. Sci. Eng. A 234–236, 758–761.

Seefeldt, M., Klimanek, P., 1998. Modelling of flow behaviour of metals by means of a dislocation–disclination reaction kinetics. Modelling Simul. Mater. Sci. Eng. 6, 349–360.

Shenderova, O.A., Brenner, D.W., 1999. Atomistic simulations of structures and mechanical properties of $\langle 0\,1\,1\rangle$ tilt grain boundaries and their triple junctions in diamond. Phys. Rev. B 60, 7053–7061.

Shizawa, K., Zbib, H., 1999. A thermodynamical theory of plastic spin and internal stress with dislocation density tensor. J. Eng. Mater. Tech. 121, 247–253.

Shu, J.Y., Fleck, N.A., 1999. Strain gradient crystal plasticity: size-dependent deformation of bicrystals. J. Mech. Phys. Solids 47, 297–324.

Soifer, Y.M., Verdyan, A., Kazakevich, M., Rabkin, E., 2002. Nanohardness of copper in the vicinity of grain boundaries. Scr. Mater. 47, 799–804.

Steinmann, P., 1996. Views on multiplicative elastoplasticity and the continuum theory of dislocations. Int. J. Eng. Sci. 34, 1717–1735.

Stumpf, H., Hoppe, U., 1997. The application of tensor algebra on manifolds to nonlinear continuum mechanics – Invited survey article. Z. Agnew Math. Mech. 77, 327–339.

Svendsen, B., 2002. Continuum thermodynamic models for crystal plasticity including the effects of geometrically-necessary dislocations. J. Mech. Phys. Solids 50, 1297–1329.

Teodosiu, C., 1967. Contributions to the continuum theory of dislocations and initial stresses. I. Rev. Roum. Sci. Techn. – Méc. Appl. 12, 961–977.

Teodosiu, C., 1969. A dynamic theory of dislocations and its application to the theory of elastic–plastic continuum. Fundamental Aspects of Dislocation Theory. NBS Special Publication 317. U.S. Government Printing Office, Gaithersburg, MD, pp. 837–876.

Teodosiu, C., Sidoroff, F., 1976. A finite theory of the elastoviscoplasticity of single crystals. Int. J. Eng. Sci. 14, 713–723.

Toupin, R.A., 1962. Elastic materials with couple stresses. Arch. Rat. Mech. Anal. 11, 385–414.

Toupin, R.A., 1964. Theories of elasticity with couple stresses. Arch. Rat. Mech. Anal. 17, 85–112.

Truesdell, C., Noll, W., 1965. The Non-linear Field Theories of Mechanics, second ed. Springer, Berlin.

Truesdell, C., Toupin, R.A., 1960. The classical field theories. Handbuch Der Physik, Band III/1. Springer, Berlin.

Valiev, R.Z., Islamgaliev, R.K., Tumentsev, A.N., 2002. The disclination approach for nanostructured SPD materials. Solid State Phenomena 87, 255–264.

Volterra, V., 1907. Sur l'équilibre des carps élastiques multiplement connexes. Ann. Ecole Norm. Sup. Paris 24, 401–517.

Wang, C.-C., Truesdell, C., 1973. Introduction to Rational Elasticity. Noordhoff, Leyden.

Wei, Y., Hutchinson, J.W., 1999. Models of interface separation accompanied by plastic dissipation at multiple scales. Int. J. Fracture 95 (1–4), 1–17.

Werne, R.W., Kelly, J.M., 1978. A dislocation theory of isotropic polycrystalline plasticity. Int. J. Eng. Sci. 16, 951–965.

Zaiser, M., 1998. A generalized composite [sic] approach to the flow stress and strain hardening of crystals containing heterogeneous dislocation distributions. Mater. Sci. Eng. A 249, 145–151.

Zbib, H.M., Rhee, M., Hirth, J.P., 1998. On plastic deformation and the dynamics of 3D dislocations. Int. J. Mech. Sci. 40, 113–127.

Zbib, H.M., De La Rubia, T.D., 2002. A multiscale model of plasticity. Int. J. Plasticity 18, 1133–1163.

Zubov, L.M., 1997. Nonlinear Theory of Dislocations and Disclinations in Elastic Bodies. Springer, Berlin.

NO. OF
COPIES ORGANIZATION

1 (PDF ONLY) DEFENSE TECHNICAL INFORMATION CTR
DTIC OCA
8725 JOHN J KINGMAN RD
STE 0944
FORT BELVOIR VA 22060-6218

1 US ARMY RSRCH DEV & ENGRG CMD
SYSTEMS OF SYSTEMS INTEGRATION
AMSRD SS T
6000 6TH ST STE 100
FORT BELVOIR VA 22060-5608

1 INST FOR ADVNCD TCHNLGY
THE UNIV OF TEXAS
AT AUSTIN
3925 W BRAKER LN
AUSTIN TX 78759-5316

1 DIRECTOR
US ARMY RESEARCH LAB
IMNE ALC IMS
2800 POWDER MILL RD
ADELPHI MD 20783-1197

3 DIRECTOR
US ARMY RESEARCH LAB
AMSRD ARL CI OK TL
2800 POWDER MILL RD
ADELPHI MD 20783-1197

ABERDEEN PROVING GROUND

1 DIR USARL
AMSRD ARL CI OK TP (BLDG 4600)

NO. OF
COPIES ORGANIZATION

ABERDEEN PROVING GROUND

30 DIR USARL
AMSRD ARL CI HC
P CHUNG
C CORNWELL
AMSRD ARL WM
M FERMEN COKER
T WRIGHT
J MCCAULEY
AMSRD ARL WM MA
W NOTHWANG
AMSRD ARL WM TA
S SCHOENFELD
AMSRD ARL WM TD
S BILYK
T BJERKE
D CASEM
J CLAYTON (10 CPS)
D DANDEKAR
M GREENFIELD
Y HUANG
K IYER
B LOVE
M RAFTENBERG
E RAPACKI
M SCHEIDLER
S SEGLETES
T WEERASOORIYA

INTENTIONALLY LEFT BLANK.